Electrochemically Regulated Polyelectrolyte Complex for Smart Wound Dressings

by

Asma S. Allababdeh

Submitted in Partial Fulfillment of the Requirements

for the Degree of

Master of Science in Engineering

in the

Chemical Engineering

Program

YOUNGSTOWN STATE UNIVERSITY

May 2022

Electrochemically Regulated Polyelectrolyte Complex for Smart Wound Dressings

Asma S. Allababdeh

I hereby release this thesis to the public. I understand that this thesis will be made available from the OhioLINK ETD Center and the Maag Library Circulation Desk for public access. I also authorize the University or other individuals to make copies of this thesis as needed for scholarly research.

Signature:

_____

Asma S. Allababdeh, Student   Date

Approvals:

_____

Dr. Byung-Wook Park, Thesis Advisor   Date

_____

Dr. Pedro Cortes, Committee Member   Date

_____

Dr. Holly Martin, Committee Member   Date

_____

Dr. Salvatore A. Sanders, Dean of Graduate Studies   Date

Abstract

Precise control over the release of drugs from wearable bioelectronic devices on wound sites, such as quantity and timing, is highly desirable in order to optimize wound treatment. The aim of this study is to obtain and characterize an electro-responsive ferrocene-chitosan/alginate polyelectrolyte complex (PEC) hydrogel that can be used as a smart wound dressing. First, chitosan/alginate PEC hydrogel was obtained as a control and characterized in terms of chemical properties and drug release kinetics. Natural chitosan (CHI) was chemically conjugated with ferrocene (Fc) moieties to create Fc-CHI. The Fc-CHI was interacted with alginate (ALG) to form Fc-CHI/ALG PEC through electrostatic interaction. The turbidity test was performed to find the optimum ratio between the Fc-CHI and ALG, thus the stoichiometric PEC hydrogel. The PEC hydrogel was characterized by Attenuated Total Reflection Fourier Transform Infrared Spectroscopy (ATR-FTIR), Scanning Electron Microscopy (SEM), Energy Dispersive X-ray Spectrometer (EDS), in addition to the swelling behavior and gel content tests. Comparative analysis of the ATR-FTIR spectra of CHI, Fc-CHI, ALG, and their mixtures indicated the formation of a polyelectrolyte complex. The SEM images showed the porosity of the PEC. The EDS analysis proved the incorporation of the Fc into the CHI by the appearance of the Fc peaks in the analysis. The PEC hydrogel showed a comparative swelling percentage to be 4400% and also showed excellent stability, proved by almost 100% gel content after incubation in phosphate buffer saline (PBS) solution. To demonstrate the drug delivery potential of the developed PEC-based wound dressing, fluorescence (FITC) and FITC-Dextran were used as model drugs. First, the drug loading and release kinetics of the PEC were studied in solution. In three days, about 83% and 61% were released of the FITC, and FITC-Dextran, respectively in PBS solution. Secondly, the drug release properties on the phantom skin surface (agarose gel) were investigated using a custom-made electrical stimulus setup incorporated with fluorescence microscopy. The release of the model drugs on the surface was tested in passive (no electrical stimulus) and active (with electrical stimulus) manners. The PEC hydrogels showed an electro-responsivity represented by increasing the intensity of the model drugs that diffused through the agarose gel under the electric stimulus. The diffusion coefficients for different drug models were estimated by analyzing images

obtained after a time series of acquisition. Based on the results, the developed Fc-CHI/ALG PEC hydrogel is prone to be an enhanced drug release upon the electrical stimulus, compared to the CHI/ALG PEC hydrogel. This indicates the presence of Fc may be able to increase the electro-osmosis and develop the enhanced stress gradient in the PEC hydrogel followed by the spontaneous drug release. The developed PEC hydrogel may be integrated with bioelectronic devices such as the smart bandage.

Table of Contents

List of Figures

List of Tables

Nomenclature

ALG	Alginate
CHI	Chitosan
Fc	Ferrocene
Fc-CHI	Ferrocene-conjugated Chitosan
PEC	Polyelectrolyte complex
FITC	Fluorescence
FITC-D	Fluorescence -Dextran
PDMS	Polydimethylsiloxane
D	Diffusion coefficient

1. Introduction

1.1. Background

Chronic wounds treatment has been a challenge worldwide. Chronic wounds affect millions of people each year and have a huge financial burden on the government of every nation. In the US, the treatment of chronic wounds costs the health care system $20-25 billion/year [1]. Wound dressings have been used to clean, cover, and protect the wound sites from the external environment, and facilitate the wound healing process. Conventional wound dressings, such as hydrogel dressings, have been fabricated to maintain a moist wound healing environment and conceal the wound [2, 3]. Some of these dressings generally provide a passive release of a drug to facilitate the healing process, which would be inadequate to complete the healing process [4, 5]. Whereas smart wound dressings monitor and react to the wound condition by having built-in smart materials, such as stimuli-responsive materials, that can provide the therapeutic drug on-demand. These smart wound dressings have been created to effectively facilitate the wound healing process [6]. Many applications on smart wound dressings have used hydrogels as drug carriers [7-10] due to their unique properties, such as high water content, biocompatibility, and biodegradability [11]. According to Bahram et al., "A hydrogel is a three-dimensional (3D) network of hydrophilic polymers that can swell in water and hold a large amount of water while maintaining the structure due to chemical or physical cross-linking of individual polymer chains" [12]. Through the chemical crosslinking, hydrogel polymeric chains are inter-connected by a covalent bond. In the physical crosslinking, hydrogel polymeric chains interact with each other physically through secondary interactions such as ionic bonds [13]. Polyelectrolyte complex (PEC) hydrogels are classified as physically crosslinked hydrogels. They are formed by the electrostatic interactions between oppositely charged polymer chains [14]. In general, PEC hydrogels can be considered as smart materials; they can be responsive to various external stimuli, such as electric field [15], temperature [16], light [17], and pH [18]. By applying a stimulus, PEC hydrogels may offer excellent properties such as on-demand drug release, which make them attractive materials for drug delivery systems. Electro-

responsive PEC hydrogels were successfully formed and stimulated and showed worthy properties in controlled drug release [19].

Chitosan (CHI) is a linear, cationic (positively charged) polysaccharide composed of N-acetylglucosamine (2-acetamido-2-deoxy-β-D-glucopyranose) and glucosamine (2-amino-2-deoxy-β-glucopyranose) units, and can be extracted from the outer skeleton of shellfish, including crab, lobster, and shrimp (see Figure 1.1 (A)) [20], and it has been widely used in biomedical applications [21]. Alginate (ALG) is a linear, anionic (negatively charged) polysaccharide that can be found within the cell walls of brown algae, and consists of β-D-mannuronic acid (M) and α-L-guluronic acid (G) residues. It also has a carboxylate functional group so it can be used to form PEC hydrogel(see Figure 1.1 (B)) [22]. ALG has been used in numerous applications such as wound healing, drug delivery, and tissue engineering due to its biodegradability and biocompatibility properties [23].
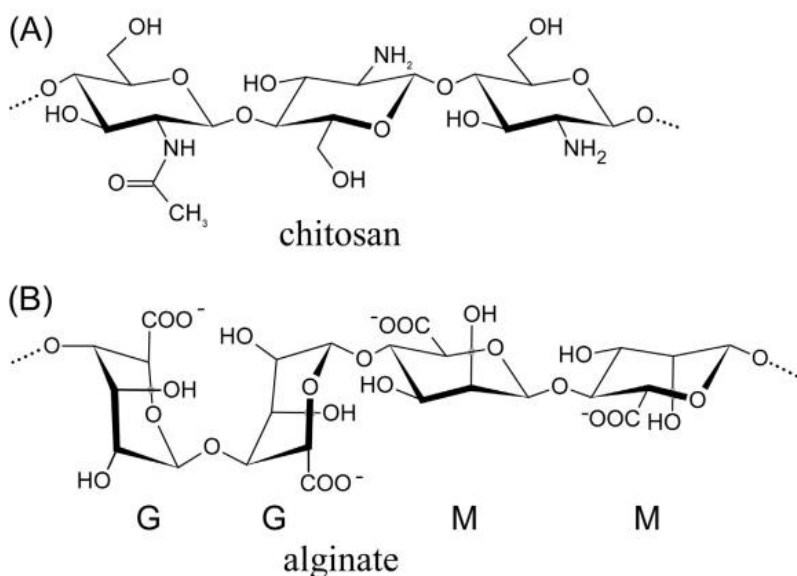
Figure 1.1. Chemical structures of (A) chitosan and (B) alginate: β-D-mannuronic acid (M), α-L-guluronic acid (G) residues [24].

In order to form a natural electro-responsive PEC hydrogel that combines the biocompatible properties of CHI and ALG, high electron transfer efficiency is required. However, the electron transfer efficiency of CHI and ALG is relatively low. This limitation can be overcome by bonding the redox mediators with the polyelectrolytes covalently through a chemical reaction [25]. Ferrocene (Fc) is a well-known redox mediator that has the property of rapid response to an electric field [26]. In this study, I hypothesize that if the ferrocene conjugated chitosan/alginate polyelectrolyte complex (Fc-CHI/ALG PEC) hydrogel is electrically responsive because of the redox probe (ferrocene), then the drug release can be controlled more efficiently under an electric field.

1.2. Objectives

The main objective of this thesis is to prepare and characterize novel electro-responsive PEC hydrogel that has proper structural strength, mechanical stability, and chemical functionality. This PEC hydrogel is controlled using an electrical field and is able to release the encapsulated model therapeutics such as FITC and FITC-D in a controlled manner, so it may provide more efficient therapy by reducing side effects and enhancing patient compliance as a smart wound dressing. The following objectives are accomplished:

- Synthesis of ferrocene conjugated CHI (Fc-CHI).
- Obtaining the charge-to-charge balanced (stoichiometric) CHI/ALG and Fc-CHI/ALG PEC hydrogels as a reference and target conditions.
- Characterizations of Fc-CHI and Fc-CHI/ALG PEC hydrogel.
- Performing drug release kinetics in passive and active (under electrical stimulus) on the surface of the phantom skin (agarose gel).

1.3. Organization

This thesis is presented in the following order:

1. A brief introduction in Chapter 1 includes the background, purpose, and benefit of the present work.
2. A literature review containing research related to the topics discussed in this thesis can be found in Chapter 2.
3. The materials and the experimental methods are provided in Chapter 3.
4. The results and discussion are presented in Chapter 4.
5. The conclusions and recommendations are presented in Chapter 5.

1.4. Scope of Work

The scope of this work is to obtain balanced CHI/ALG PEC hydrogel as a reference and starting point, and then electro-responsive Fc-CHI/ALG PEC hydrogel. Different amounts of ferrocene were conjugated in the chitosan and tested to find the

most efficient condition regarding electrochemical functionality and mechanical stability. In order to characterize the PEC hydrogels, turbidity measurements, Attenuated Total Reflectance Fourier Transform Infrared Spectroscopy (ATR-FTIR), Scanning Electron Microscopy (SEM) with energy dispersive X-ray spectrometer (EDS) analysis, a swelling behavior test, and a gel content test were performed. Two model drugs were used in order to characterize the release behavior in solution, and on the surface of the phantom skin (agarose gel) in two conditions: passive (sustained) release and active (electrical stimulus).

2. Literature Review

2.1. Wound dressings

For a wound to heal, the major protocol is to have successful wound management. Wound management is a challenge worldwide. An important part of wound management is knowing the potential dangers of wound infection such as extreme fever [27]. However, wound dressings can facilitate and promote the wound healing process; also, they help to maintain appropriate conditions around the wound, therefore reducing the chance of wound infection. The different types of wound dressings will be reviewed here.

2.1.1. Conventional wound dressings

A proper wound dressing can provide protection and decontamination in addition to maintaining the moisture of the wound area and preventing infection [28]. Traditional wound dressings such as bandages and cotton can be generally used to cover the wound and absorb the exudates, which may be inefficient in dealing with large, wet, and deep wounds because they lack the property of maintaining moisture. Conventional wound dressings have been developed to manage the wound conditions and promote the wound healing process. Hydrogel, foam, and hydrocolloid dressings are types of conventional dressings [29]. This section will focus on hydrogel wound dressings.

Various hydrogel wound dressings have been fabricated and showed a significant improvement in the wound healing process [30]. These dressings can be formed as a film [31] or formed *in situ* [32]. The ability of hydrogels to swell is an important factor in terms of increasing the ability to absorb wound exudates as well as maintaining a moisturized environment around the wound site. It was reported that a natural, nontoxic film hydrogel dressing, composed of methoxyl pectin, gelatin, and carboxymethyl cellulose, was fabricated and incubated in phosphate buffer saline (pH 7.4) in order to test the water uptake ability [33]. The weight of the swollen hydrogel was found to be 1.9-fold the initial weight, which exhibits relatively low swelling behavior, compared to another study that presented the hydrogel dressing composed of chitosan/γ-poly (glutamic acid). The results showed that the hydrogel dressing reached 10-fold the initial weight after incubation in water [31]. Another study reported a sacran hydrogel as a

wound dressing with a swelling percentage of 1900% which is equivalent to 19-fold the initial weight after it was incubated in water [30]. In order to show the performance of this dressing in promoting the wound healing process, *in vivo* studies were conducted by creating wounds on mice that were divided into two groups: non-treated (as control) and sacran hydrogel treated. The wounds were monitored for 12 days (see Figure 2.1). On the sixth day, the wound closure percentage for the control was 40%, while it was 80% for the treated wounds. By day 12, the wound closure percentage was 88% and 95% for control and treated wounds, respectively. These results demonstrated that the sacran hydrogel dressing may accelerate the wound healing process.
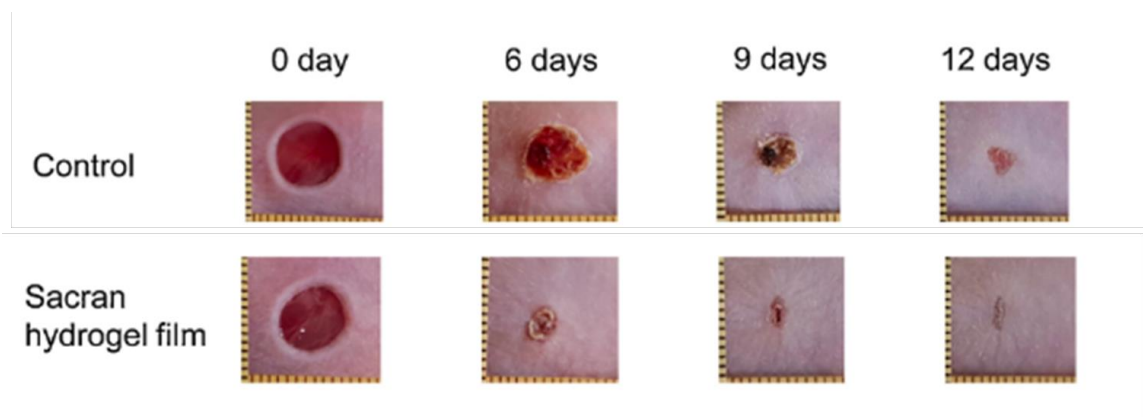
Figure 2.1. *In vivo* wound healing study of sacran hydrogel compared to non-treated wound.

To have a comfortable and smooth dressing covering the wound area, hydrogel wound dressings could also be formed *in situ*. A study presented biodegradable and nontoxic *in situ* forming hydrogel wound dressing, based on oxidized alginate and gelatin [32]. The oxidized alginate was easily cross-linked with gelatin using borax to present 'in situ forming hydrogel.' The fluid uptake of the hydrogel was found to be 90% of its weight, which is comparative to the previous work showing a similar uptake ability [30].

Furthermore, in terms of proper wound dressing to provide medications that accelerate the healing process, some of the hydrogels were loaded with drugs (e.g., antibiotics) and vitamins. For example, a research work reported ALG hydrogel dressing that was loaded with vitamin D3 [34]. Vitamin D3 was selected in the study, due to its

role in enhancing the proliferation of both fibroblasts and keratinocytes, which are two primary cell types involved in skin wound healing. To demonstrate the capability of the loaded-ALG dressing to promote the wound healing process, an *in vivo* study was conducted (on a rat) as shown in Figure 2.2 (A) and (B). The wound closure for the wounds that were treated with the loaded-ALG dressing had a higher percentage compared to the gauze treated wounds, as follows: The average wound closure for the loaded dressing was 71.42% and 92% on days 7 and 14 post wounding, respectively while the average wound closure for the control on the 7th and 14th days was 42% and 64.8%, respectively (see Figure 2.2 (C)). A similar study presented a wound dressing based on ALG hydrogel that was incorporated with naringenin, a flavonoid in the flavanones subclass that can display strong anti-inflammatory and antioxidant activities[35]. The *in vitro* study that was conducted on a rat showed that the wound closure was 68% and 95% of hydrogel-treated wounds on day 7 and day 14 respectively. Conversely, the wound closure was 43%, and 48% of gauze-treated wounds on day 7 and day 14 respectively. According to the results from the presented studies, the loaded hydrogel dressings accelerated the wound healing process by providing therapeutics on top of the hydrogel-moistened environment.

In terms of the release rate of the therapeutics drugs from the dressings, some of the dressings were able to provide the drug over a long period, while some of them were releasing the drug within hours. In a study, Polyvinyl alcohol/polyethylene glycol hydrogel that is elastic and swellable was fabricated as a wound dressing. It was loaded with Asiaticoside, which is rich in Centella Asiatica [36]. The study showed that more than 90% of the drug was released within 12 hours. By comparison, another study showed the release of simvastatin (a cholesterol-lowering antihyperlipidemic, that showed potential in healing diabetic wounds) from alginate-pectin hydrogel dressing was sustained and slow over more than three days [37]. This dressing allowed the release of the drug on the wound site for a longer time compared to the Polyvinyl alcohol/polyethylene glycol hydrogel dressing [36]. exposing the wound sites to a small amount of the therapeutic drug for a longer time prevented infections and more effectively promoted the healing process.

Figure 2.2. (A) Microscopic image of the wound model created on the dorsum of the rat. (B) Image of the wound dressing. (C) Images of the healing process for the control and the vitamin D3 loaded dressing at different times [34].

2.1.2. Smart wound dressings

Dressings that can sense and react to the wound conditions are called smart wound dressings. These dressings have structural materials such as hydrogels that also can be responsive to wound conditions[38]. Any elevation of the physicochemical and physiological parameters of the wound sites, including pH, temperature, and moisture, will stimulate the dressing to provide the therapeutic drugs and therefore more effectively promote wound healing. It was reported that a smart wound dressing provided an aminoglycoside antibiotic based on the temperature of the wound site [39]. The structure of the wound dressing was as follows: It has a double-layer structure. The top layer is composed of polydimethylsiloxane-encapsulated flexible electronics integrated with a temperature sensor and ultraviolet (UV) light-emitting diodes. The lower layer is a UV-responsive hydrogel which is composed of poly-ethylene glycol, shown in Figure 2.3 (A). The wound temperature was monitored by a sensor and transmitted to portable equipment (e.g., smartphone) via Bluetooth. When the temperature exceeded 38°C

9

(which is a sign of pathogenic infection), the UV light was turned on to stimulate the hydrogel to release the antibiotic *in situ*, as shown in Figure 2.3 (B).
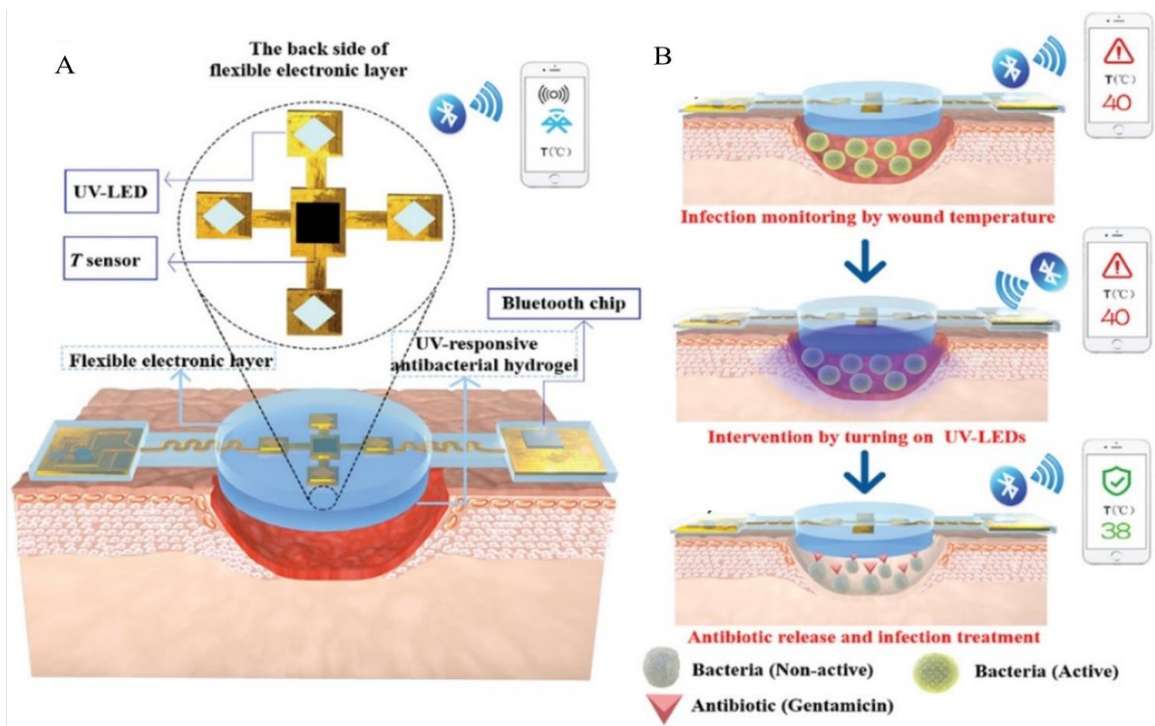
Figure 2.3. (A) The structure of the smart wound dressing. (B) Conceptual view of the system, the infection monitoring and the on-demand treatment [39].

Another work presented a flexible dermal patch with heating elements for on-demand drug delivery[7]. The patch was composed of micropatterned gold heating elements and a calcium-alginate sheet, which can be loaded with thermo-responsive drug microcarriers. N-Isopropylacrylamide (NIPAM) has been used to fabricate the thermo-responsive particles because it has responsivity to temperature changes. At a temperature below 32° C, it becomes hydrophilic, and above its critical point (≈ 32 °C), it becomes hydrophobic. The heating element was connected to a microcontroller to have the patch temperature controlled. From this structure, an electrical current can be applied to the flexible heater that controls the patch temperature and releases the drug on demand. In the previous work [39], the temperature was monitored through a sensor connected to portable equipment and provided a specific reading about the wound temperature condition, which proved to have a more advanced structure.

10

The healthy skin is acidic, in the range of pH between 4 and 6. Depending on the infection types the pH elevates from the normal range and becomes alkaline [40]. Some smart wound dressings have monitored the pH environment of the skin to provide the drugs on-demand. A low-cost and flexible dermal patch was fabricated that released tobramycin antibiotic depending on the pH value [1]. The patch structure can be seen in Figure 2.4 (A). A drug reservoir was located on the top. A thin membrane separated the drug reservoir from the pH-responsive hydrogel and the two pumps on the sides. The aqueous drug remained in the reservoir because the pumps and output channels were made of polydimethylsiloxane (PDMS, a hydrophobic polymer). The last layer was a porous membrane that allowed the drug to pass into the skin. The pH-responsive hydrogel that was used in this wound dressing was composed of poly (methacrylic acid-co-acrylamide). When the hydrogel was exposed to high pH (as a result of an infected wound), the carboxyl group of the hydrogel was ionized to $-COO^-$, thus the electrostatic repulsion was increased in the chains of the hydrogel. The deprotonated carboxyl groups led to swelling of the hydrogel against the deflectable membrane, allowing the antibiotic to be pumped out. Conversely, when the pH was decreased, the $-COO^-$ was combined with H^+ and formed -COOH; therefore, the electrostatic repulsion decreased, and the hydrogel shrunk to prevent the antibiotic from being released. (Figure 2.4 (B) and (C))
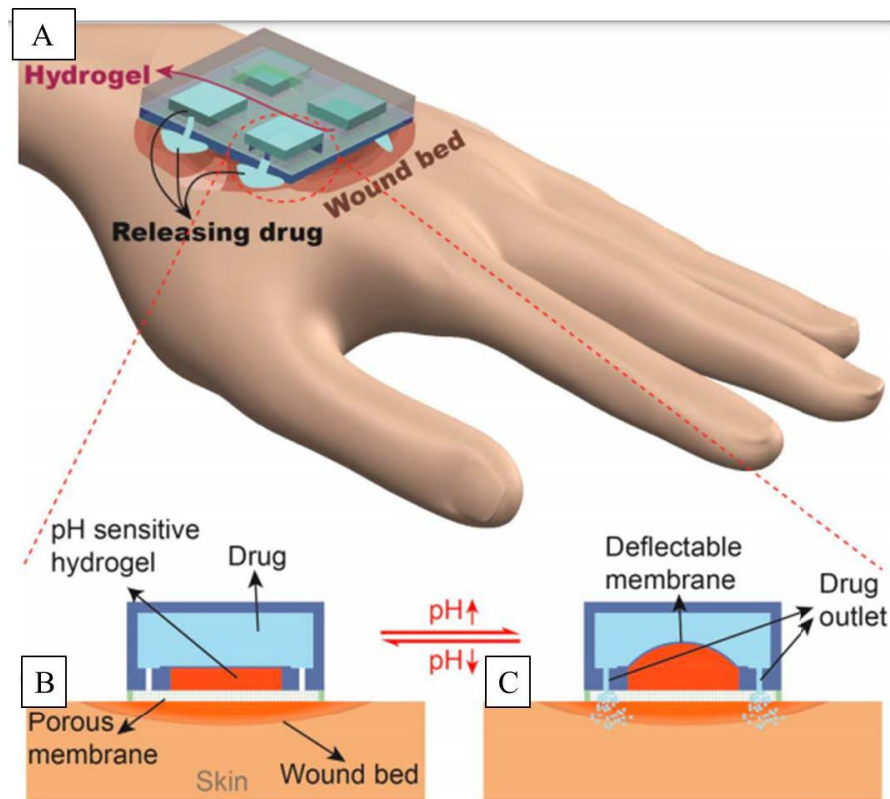
Figure 2.4. (A) The structure of the smart wound dressing. (B) No drug release at the non-infected area (pH is low). (C) In an infected area (pH is high), the pH- responsive hydrogel swells against the deflectable membrane, allowing the drug to be pumped out [1].

The *in vitro* experiment was performed using *P. aeruginosa*. The pump was releasing the tobramycin antibiotic for a full 24 hours. The results were compared to a control sample that had the same number of bacteria but without the pump releasing the antibiotic. The images in Figure 2.5. (A) and (B) show the reduction of the bacteria after the pump-assisted antibiotic treatment. The starting concentration for the bacteria culturing was 4.5×10^7 CFU/ml. After 24 hours of incubation, the concentration increased to 47×10^7 CFU/ml for the bacteria that were not exposed to the antibiotic, but it was decreased to 0.8×10^7 CFU/ml for the antibiotic-treated bacteria, as shown in Figure 2.5 (C). Therefore, a 58 times reduction in the bacteria was found, which is evidence of this dressing's ability to facilitate the healing process and treat chronic infections.
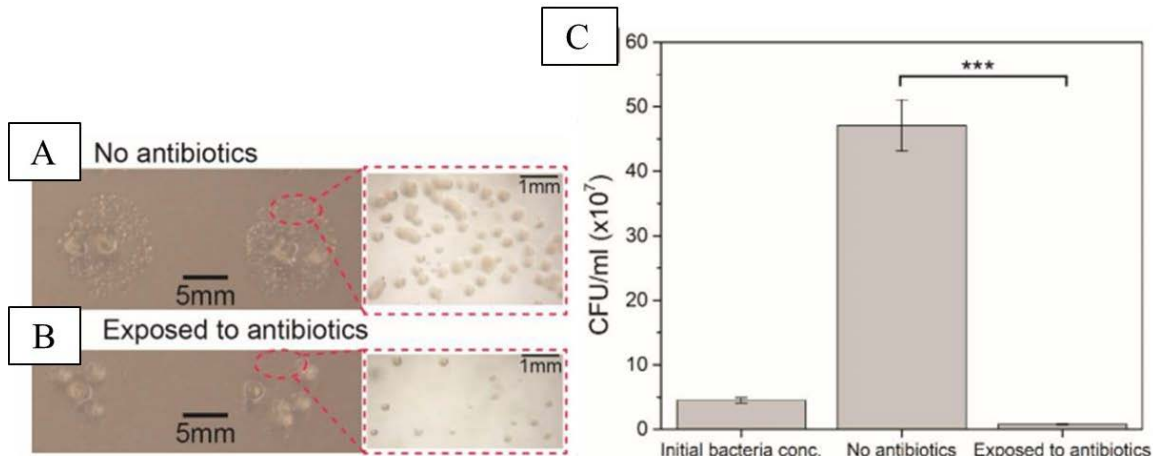
Figure 2.5. (A) The bacteria culture before exposure to antibiotic is released from the pump. (B) The bacteria after exposure to the antibiotic is released from the pump. (C) The concentration of the bacteria initially, without antibiotic exposure and with exposure to antibiotics.[1]

In another study, Methacrylic acid hydrogel was used as a pH-responsive wound dressing [38]. Silver nanoparticles (AgNPs) were encapsulated inside the hydrogel because of their antibacterial properties. The drug delivery system was able to sense the pH and release the AgNPs when the wound environment changed from acidic to alkaline. The results showed that the hydrogel was releasing AgNPs under alkaline conditions (pH= 7.5–10) and restricting the release under acidic conditions (pH= 4). (See Figure 2.6)
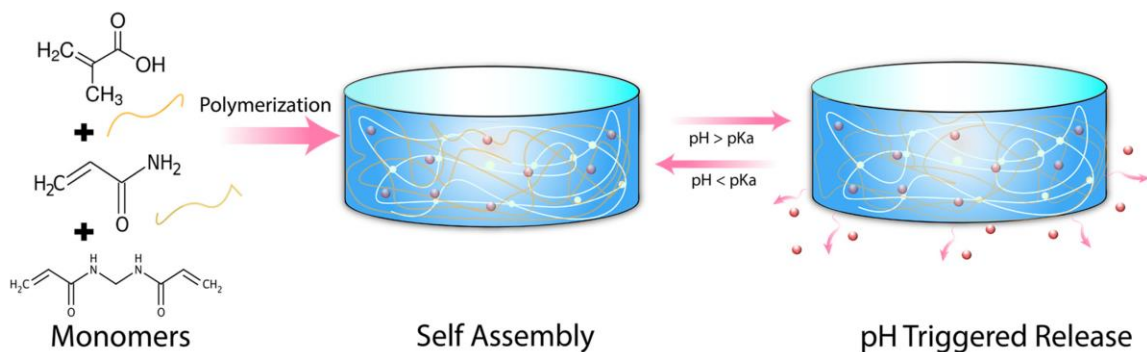
Figure 2.6. The drawing shows the methacrylic acid hydrogel synthesis and the active release of the drug [38].

2.2. Hydrogels

Hydrogels are polymeric networks that are produced by a reaction of one monomer or more. These hydrogels have a high ability to swell and retain a large amount of water within pores [41-43] and have a soft consistency similar to natural tissues [44]. Along with these properties, they are biocompatible and biodegradable [45, 46]. For these reasons, hydrogels have been used in medical applications, including tissue engineering [47] and bioprinting [48]. Moreover, they are widely used for different kinds of wound dressings [49] and drug delivery systems [38]. A variety of natural, synthetic, and semi-synthetic polymers are used to form hydrogels. Through physical or chemical crosslinking (see Figure 2.7) [50], these hydrogels have different properties in terms of swelling behavior, pore size, and mechanical strength [35, 51-53]. PEC hydrogels are classified as physically crosslinked hydrogels and can be natural, synthetic, or semi-synthetic. This is specified in the following section.
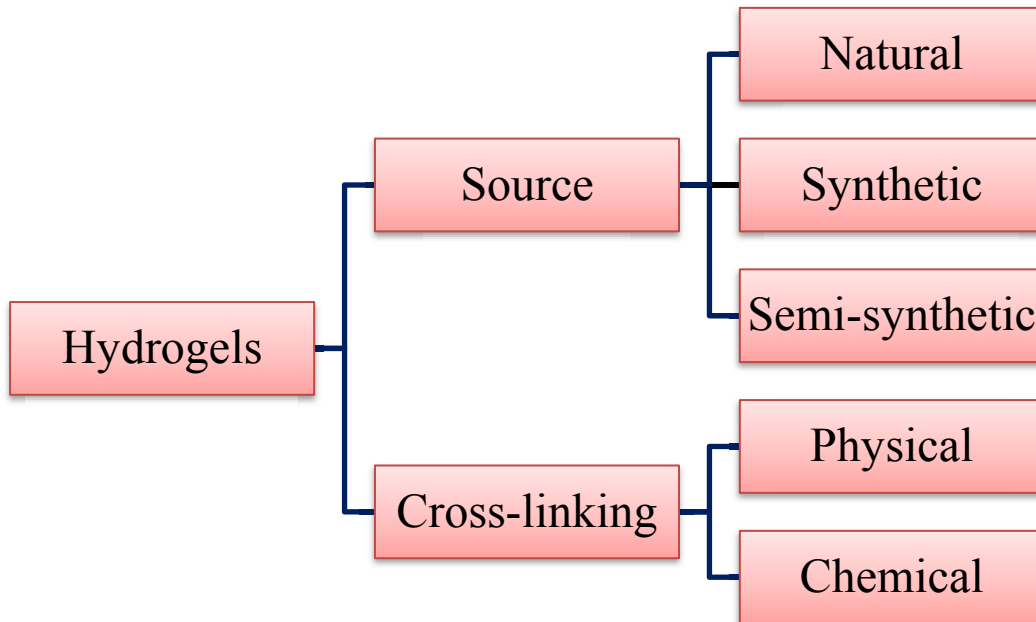
Figure 2.7. Classification of hydrogels.

2.3. Polyelectrolyte complex hydrogels

2.3.1. Basics of PECs

Polyelectrolytes are macromolecules with several repeating chain units that have a large number of functional groups. These groups are charged or can be charged under specific conditions (e.g., pH) [54]. PEC hydrogels are formed by mixing oppositely charged polyelectrolytes (polyanion with polycation) in an aqueous solution (as described in Figure 2.8). The strong electrostatic interaction between two electrolyte chains is the main driving force to form the PEC hydrogels [55]. Both PEC hydrogels and polyelectrolyte multilayers have similar physical and chemical properties in terms of their internal and physical structures [56]. These PEC hydrogels are biocompatible and can be responsive to changes in surrounding conditions [57].
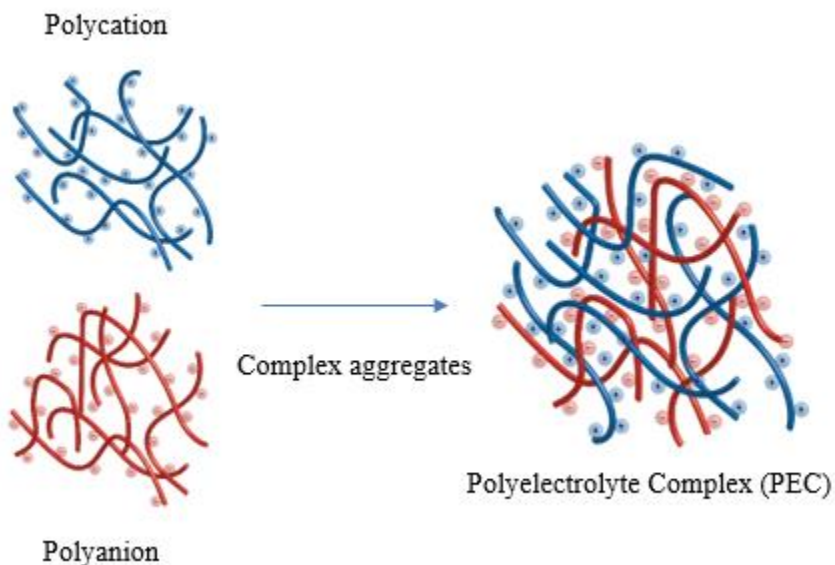
Figure 2.8. PEC hydrogels formation.

When it comes to stability and formation of the PEC, there are several important factors such as molecular weight [58], concentration [59], mixing ratio of the polyanion and polycation molecular [60], mixing order [61], and duration of mixing [62]. Moreover,

the pH and temperature of the polyelectrolytes solutions are the most important factors because changes in pH and temperature may result in protonation or deprotonation of the functional groups of the polyelectrolytes, which affects the PEC formation [55, 63]. The effect of mixing different ratios of the polyelectrolytes on the formed PEC was studied in a research work [64]. CHI/ALG PEC hydrogels were prepared in different ratios of CHI and ALG as presented in Table 2.1.

Table 2.1. Water uptake ability of different ratios of CHI/ALG PEC hydrogels [64]**.**

Sponge type	Mixing ratios		Water uptake ability (%)
	ALG	CHI	
CHI3/ALG1	1	3	4290
CHI2/ALG2	2	2	3806
CHI1/ALG3	3	1	1218

From the results, the water uptake ability for the CHI3/ALG1, CHI2/ALG2, and CHI1/ALG3 was 4290%, 3806%, and 1218%, respectively. It showed how the mixing ratio affected the interaction between the CHI and ALG. The fibrous networks contained in each PEC hydrogel were different and therefore affected the ability of each hydrogel to retain water within pores [64].

Another work presented a study on the characteristics of CHI/ALG PECs composed of different polymer ratios. Nine different ratios were prepared by changing the percentage of ALG in the samples, starting with 20% ALG and ending with 50% ALG [60]. The FT-IR analysis showed that the degree of the electrostatic interaction between the polymers was affected by changing the ratio of CHI and ALG. The FT-IR spectra of the CHI, ALG, and the CHI/ALG complex are shown in Figure 2.9. A strong peak was seen for CHI at 1569 cm^{-1} combined between amide I and amide II groups. The absorption bands of ALG were seen at 1605 and 1410 cm^{-1} and represented asymmetric and symmetric stretching vibrations of carboxylate groups, respectively. The disappearance of these peaks or the appearance of new peaks were observed in the polyelectrolyte's blends spectra, indicating the ionic bond was created between ALG and

CHI. New peaks were observed at 1580 cm^{-1} and 1730 cm^{-1} in all the prepared PEC ratios. The peak at 1730 cm^{-1} represented the asymmetric stretching of carboxylate groups, which demonstrated PEC formation. When the percentage of ALG was ≥ 38 in the sample, the peak intensity at 1398 cm^{-1} was observed, demonstrating that stronger electrostatic interaction occurred in the samples that have a ratio closer to 1 (50% ALG, 50% CHI). The FT-IR analysis demonstrated that the mixing ratio affects the PEC formation as well as the strength of the electrostatic interaction between the polyelectrolytes.
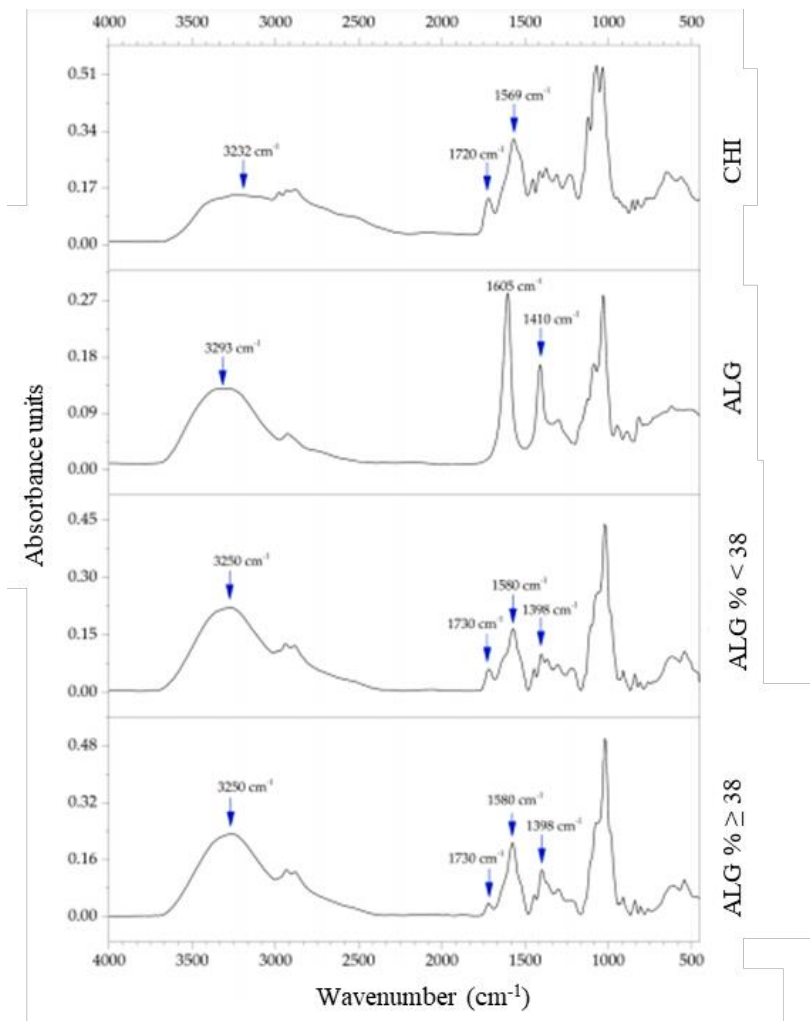
Figure 2.9. The FT-IR spectrum of CHI, ALG, and different ratios of CHI/ALG PEC hydrogels. [60]

In a study on the effect of the polyelectrolyte concentrations on the PEC formation [59], CHI/ALG hydrogel was prepared using a range of concentrations (0.5–2 wt. % for CHI and 0.5–2.5 wt. % for ALG). After mixing, a gel-like opaque figuration appeared (Table 2.2). The interaction between the CHI and ALG was changing as the concentration was adjusted. The PEC which composed of 2 wt. % CHI and 2.5 wt % ALG were used for the characterization due to the higher turbidity of the PEC solution. This indicated that the interaction between the polyelectrolytes was charge-charge balanced [59].

Table 2.2. Images of CHI/ALG PEC were prepared with different concentrations of the CHI and ALG in an aqueous solution [59]**.**

Also, research was conducted to study the effect of the molecular weight of the polymers on the properties of the PEC. The obtained PEC samples were composed of polyvinylamine (PVAm) and carboxymethyl cellulose (CMC). The molecular weight (Mw) of PVAm was 150 kDa and three different Mw of CMC with differing degrees of carboxymethylation (DS) were used (Mw/DS, 90 kDa/0.7, 250 kDa/0.7, and 250 kDa/1.2). The samples were prepared by changing the ratio between CMC and PVAm.

According to the tensile strength and modulus tests (as shown in Figure 2.10), the mechanical strength of the PEC hydrogels was increased with decreasing the molecular weight of CMC. Due to the stiffness of the cellulosic chains, shorter ones tend to maximize the intermolecular interactions during PEC formation [58].
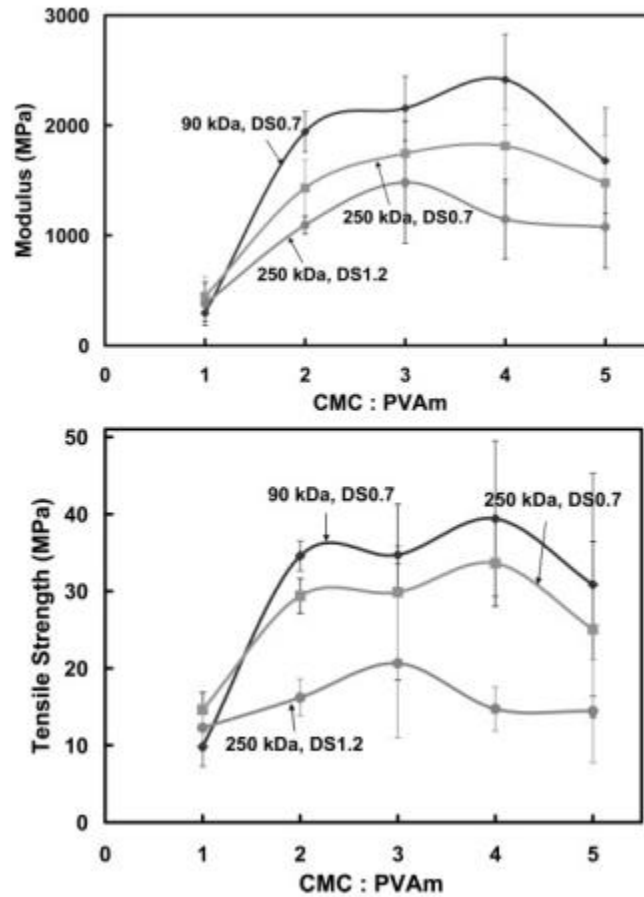
Figure 2.10. The effect of CMC Mw on the mechanical properties of PEC hydrogels **[58]**.

The mixing ratio between positively and negatively charged polyelectrolytes resulted in either a stoichiometric PEC (that has a net charge equal to zero and is insoluble) or a nonstoichiometric PEC (that has an excess of one charge, positively or negatively, and is subsequently more hydrophilic and soluble PEC) [65]. Several characterization methods are used to determine the optimal ratio between the charge-to-charge balanced polyelectrolytes, such as the turbidity test [66], and potentiometric and conductometric titrations [67]. The optimal ratio between two polyelectrolytes can be

found when the PEC is more turbid and has a viscosity close to the viscosities of the polyelectrolyte's solutions. The turbidity test was performed on the PEC hydrogels composed of anionic tragacanth gum (TG) and cationic CHI with or without the addition of anionic xanthan gum (XG) as shown in Figure 2.11. The different ratios of CHI, TG, and XG were tested; the stoichiometric PEC was found with the highest turbidity with a value of 119 NTU for TG/CHI PEC and 129 NTU for TG/XG/CHI [68].
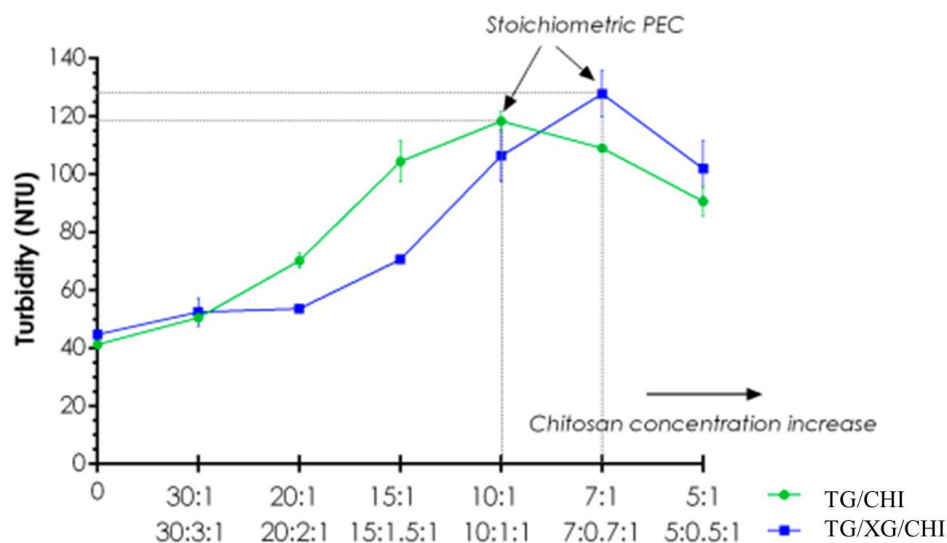
Figure 2.11. The turbidity curves for TG/CHI and TC/XG/CHI PEC hydrogels [68].

2.3.2. Types of PEC

PEC hydrogels can be natural, synthetic, or semi-synthetic. Natural PEC hydrogels are composed of polymers derived from natural sources, such as chitosan, sodium alginate, gelatin, collagen, carrageenan, pectin, xanthan gum, and hyaluronic acid [69]. Because natural PEC hydrogels are biocompatible, they are attractive materials for biomedical applications, drug delivery systems, and tissue engineering [70-72]. It was reported that the natural CHI/gum-arabic PEC hydrogel has been fabricated as a drug delivery system for oropharyngeal candidiasis treatment. The PEC was loaded with nystatin which is an antibiotic (obtained from *Streptomyces noursei)* that could be used

for the treatment of oropharyngeal candidiasis. The drug release behavior of the PEC was investigated; a burst effect followed by a moderate release profile was found (55% of the drug was released by the second hour and 84% was released within 24 hours). Also, the loaded PEC showed antimicrobial activity against *Candida albicans* and *Pichia kudriavzevii*. According to the *in vitro* studies, these results qualified the PEC to be used in drug delivery systems [73]. Another natural PEC hydrogel composed of CHI and hyaluronic acid was obtained as a drug carrier for the delivery of doxorubicin (DOX), which is a drug that can slow or stop the growth of cancer cells [74]. When the release behavior of the PEC was tested, there was evidence that DOX was released slowly over 4 days and no burst release occurred in comparison with the previous example [73]. This indicates a benefit to providing the drug for a longer time, therefore enhancing the treatment condition for which the PEC is used. However, even with all of the beneficial properties of natural PEC hydrogels as drug carriers, they are nonetheless limited because of their poor mechanical properties [75].

Synthetic PEC hydrogels are formed when two synthetic polymers interact with each other through the ionic bond. There are various synthetic polymers, such as poly (vinyl alcohol), polyacrylic acid, poly (tetrafluoroethylene), poly (vinyl chloride), and poly (ethylene oxide) [76]. The PEC formation between polyacrylic acid and poly (diallyl dimethylammonium chloride) has been reported [77], also a complexation between the oppositely charged PNIPAM-b-poly (acrylic acid)-b-PNIPAM and poly (2-(dimethylamino) ethyl methacrylate) has been obtained and resulted in a form of PEC that is responsive to the temperature change due to sensitivity of PNIPAM to the temperature. The main advantage of synthetic PEC hydrogels is that they have excellent mechanical strength and tunable stiffness [75]. However, synthetic hydrogels may need to enhance their biocompatibility. The lack of biocompatibility is a primary disadvantage of synthetic PEC hydrogels compared to their natural forms [78].

The complexation between oppositely charged natural and synthetic polymers results in semi-synthetic PEC hydrogels. These hydrogels have overcome the limitations between the low mechanical strength in the natural PEC hydrogels and the low biocompatibility in the synthetic ones. Therefore, they have been widely used in the biomedical field for drug delivery systems [79-81]. It was reported that

CHI/tripolyphosphate PEC hydrogel was formed in a novel method, with mechanical strength that increased 10 times compared to the conventional method. The novel method included increasing the crosslinking time between the CHI and tripolyphosphate, which resulted in the formation of a homogeneous PEC with high mechanical strength [79]. When this PEC hydrogel was tested as a drug carrier using FITC-Dextran as a model drug, the results indicated that the FITC-Dextran was released from the PEC in a sustained manner for 24 hours. This release behavior is comparative to the release behavior of natural PEC hydrogels [73].

2.3.3. Types of release

The encapsulated drugs in PEC hydrogels can be released in a sustained manner (no stimulus) over a period of time. However, some of the PEC hydrogels can be responsive to different types of stimuli, such as pH environment, temperature, light, and electric field, allowing the release of the drugs at a controlled rate or specific time (on-demand). The forms of the responses can be shown as swelling, shrinking, or eroding of the PEC network. The types of release are reviewed in this section.

2.3.3.1 Passive release

Because PEC hydrogels have relevant properties, such as biocompatibility and the ability to maintain water within pores as required for drug delivery systems, a variety of PEC hydrogels have been developed with loaded therapeutics to provide the drugs *in situ* for wound dressing applications and treatment of different diseases (e.g., cancer). The sustained release allows delivery of the drug over a period of time without providing any stimulus. Research work presented a study on the sustained release of Rabeprazole Sodium (as a model drug) from O-carboxymethyl chitosan/carbopol PEC hydrogel [82]. O-carboxymethyl chitosan/carbopol PEC hydrogel was crosslinked with calcium to show the effect of the concentration of the crosslinker, the composition of the PEC, and the crosslinking time on the sustained release behavior of the PEC hydrogel. The results indicated that the increase in the concentration of the crosslinking agent, from 1% (w/v) to 8% (w/v), led to reduced drug release (Figure 2.12 (A)).

22

The release rate of Rabeprazole Sodium increased with the increase in O-carboxymethyl chitosan concentration. The PEC hydrogels that have low concentrations of O-carboxymethyl chitosan tend to be fragile, so the rapid release of the encapsulated drug was observed in the first 4 to 5 hours (Figure 2.12 (B)). Figure 2.12 (C) shows the effect of the crosslinking time on the drug release. The samples showed faster release when the PEC hydrogels were allowed to crosslink the calcium chloride for 15 minutes, and slower release for the samples that crosslinked for 30 and 45 minutes. The short time release was due to the insufficient interaction between the calcium chloride and PEC hydrogels. Therefore, a weaker PEC matrix was formed, and the release of the drug was faster. Overall, in this study, the sustained release of Rabeprazole Sodium in all the conditions was over a period of 10 hours. While in another study that investigated the sustained release of immobilized bone morphogenetic protein-2 (BMP-2) from chitosan–hyaluronic acid PEC scaffolds, the BMP-2 was released in a sustained manner for more than four weeks. The longer release time was attributed to the high loading efficiency of the BMP-2, which was immobilized in the PEC hydrogels by electrostatic interaction [83].
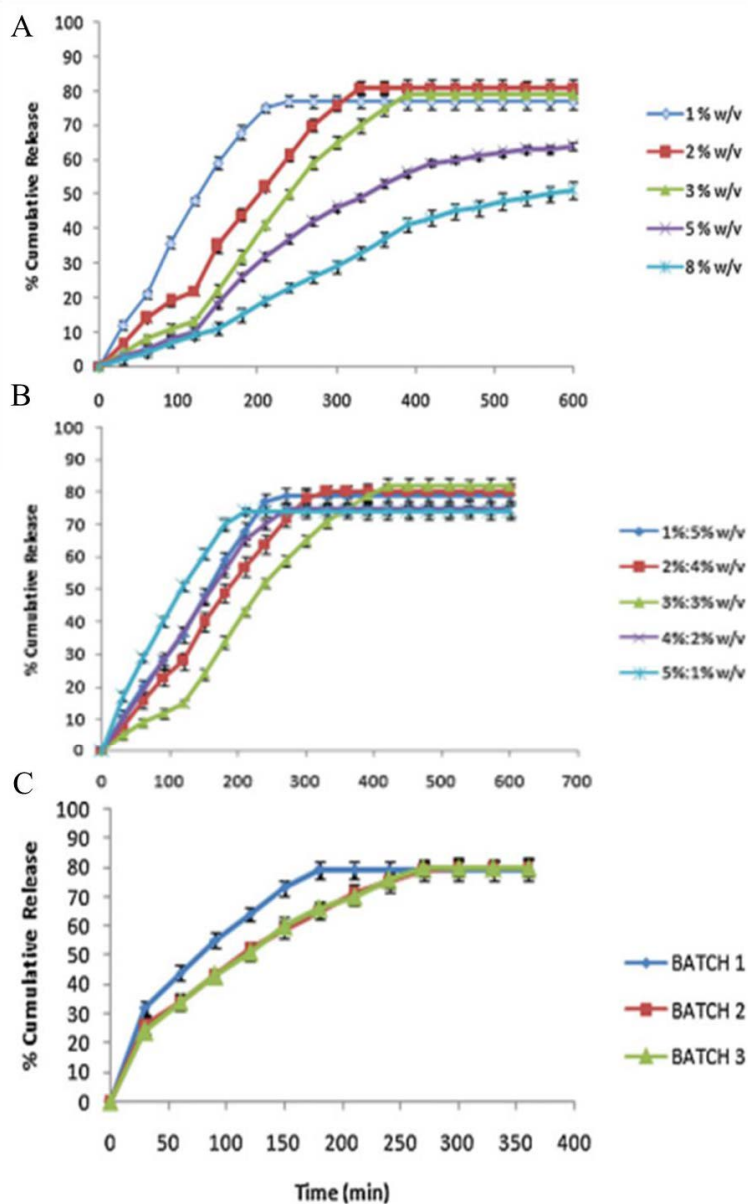
Figure 2.12. (A) the effect of the crosslinker concentration on the release profile of the drug. (B) the effect of O-carboxymethyl chitosan: Carbopol composition on the release profile of the drug. (C) the effect of the crosslinking time on the release profile of drug from the PECs (Batch (1) 15 min; Batch (2) 30 min; Batch (3) 45 min) [82].

The sustained release of CHI/ALG PEC hydrogels using different ratios of the polyelectrolytes was also studied [64]. The ratios were prepared as follows: (1:1), (3:1), and (1:3) of (CHI: ALG). Curcumin was used as a model drug due to its pharmacological properties such as anti-inflammatory, antimicrobial, antiviral, anticancer, and

antioxidant. The curcumin-loaded PEC hydrogel (Figure 2.13 (A)) was prepared by mixing the CHI solution containing curcumin with the ALG solution. The loaded PEC hydrogels were used to test the sustained drug release. The sustained release of curcumin was tested for a period of 20 days. Figure 2.13 (B) shows the drug release behavior of the 3 different ratios of the PEC hydrogels: 50% and 70% were respectively released from (1:1) and (3:1) ratios. From the (1:3) ratio, 80% of the curcumin was released in 3 days. The ratio (1:1) offered preferable sustained release because this sample released lower amounts of curcumin compared to the other ratios. Therefore, it can provide the drug for a longer time.
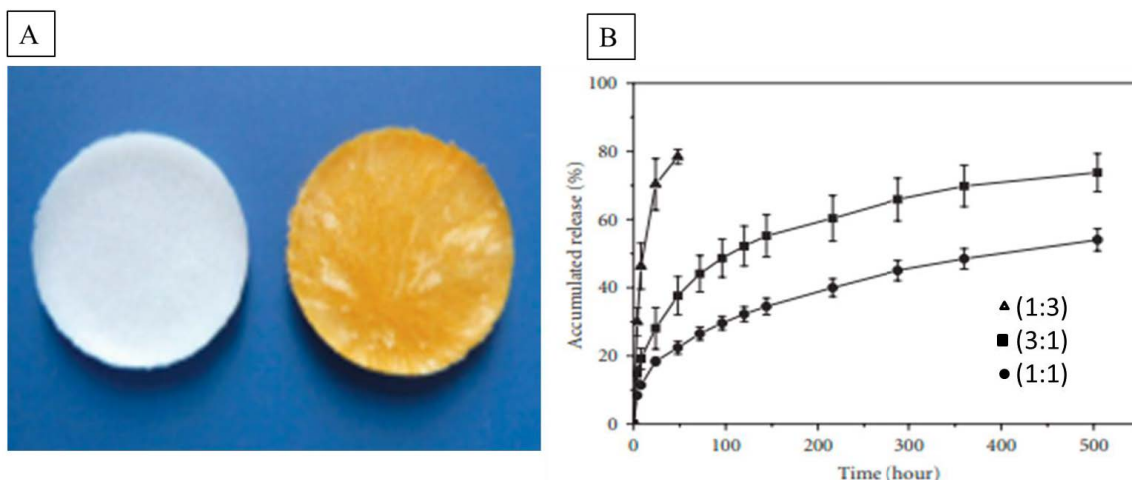
Figure 2.13. (A) Photograph of the CHI/ALG PEC hydrogel. (Left, pure PEC hydrogel /right, PEC hydrogel loaded with curcumin). (B) The drug release behaviors of different ratios of CHI/ALG PEC hydrogels [64].

2.3.3.2 Active release: pH

The condition of the functional groups of the polyelectrolytes plays a major role in the responsivity of PEC hydrogels. Protonation or deprotonation of the functional groups at different pH values leads to distribution in the electrostatic interactions between the cationic and anionic polyelectrolytes. Therefore, a change in the swelling behavior of the PEC occurs. For example, a novel dual pH-responsive PEC hydrogel was formed by mixing the polyelectrolytes: poly (2-(dimthylamino) ethyl methacrylate) (PDMAEMA)

and poly (acrylic acid) (PAAc). The hydrogel was dually pH-responsive; it was stable in a neutral pH environment and can be swollen in either acidic or alkaline pH environments. The swelling ratio curve versus the pH had a U shape as can be seen in figure 2.14 [84].
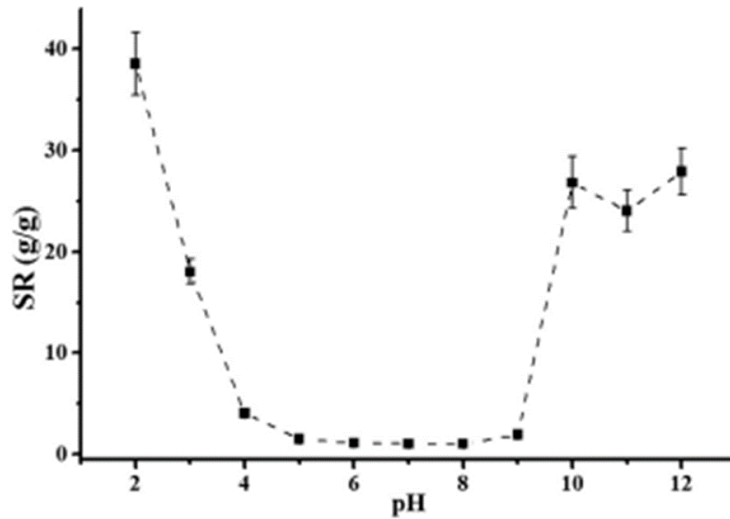
Figure 2.14. The swelling behavior of DMAEMA/ PAAc PEC in buffer solution with different pH values at room temperature [84].

The mechanism of the dual pH- responsivity was that a portion of PAAc at lower pH was deprotonated while the PDMAEMA remained in a charged form as shown in Figure 2.15. The charged PDMAEMA chains expanded and swelled due to the partly decomposed PEC hydrogel. As the pH decreased, the portion of the neutral PAAc and charged PDMAEMA increased thus causing the higher swelling ratio of the PEC hydrogel.
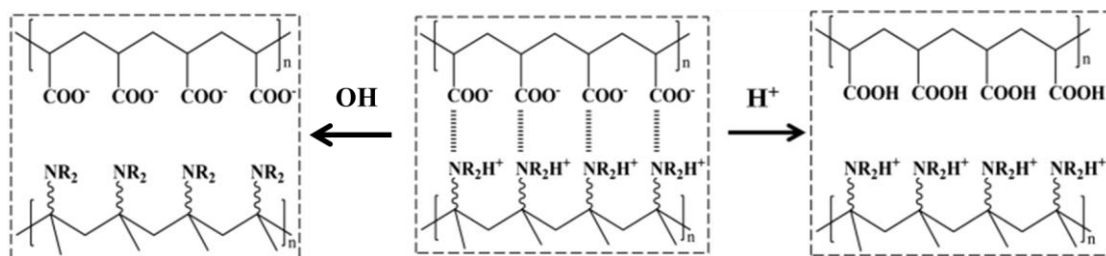
Figure 2.15. The mechanism of the responsivity of the PEC hydrogel to strong acid and strong base [84].

In another study, CHI and Xanthan were used to prepare a pH-responsive PEC hydrogel. The swelling behavior was tested in NaOH or HCl solution. In NaOH solution (pH 10-12), the PEC hydrogel swelled. The Xanthan has carboxyl groups, and the CHI has amino groups. When the PEC hydrogel was incubated in NaOH solution, the amine group on the CHI chain was deionized and the carboxyl group maintained the negative charge. Therefore, the bond between the electrolytes broke and allowed the hydrogel to be swollen [18]. Another study with the crosslinked CHI/ALG PEC showed a similar trend [24]. The PEC hydrogel was noted to have a higher swelling ratio at pH 3.5, and a lower swelling ratio at pH 9. This behavior can be explained by the protonation and deprotonation of amino groups in CHI and carboxylate groups in ALG.

2.3.3.3 Active release: Electro

Electro-responsive PEC hydrogels offer unique advantages for controlled drug release; they can provide the drug on demand when exposed to an electric field. The drug release from the electro-responsive PEC hydrogels resulted from the electro-induced changes in the hydrogels [15]. An electro-responsive hydrogel was prepared with hyaluronic acid (HA) and poly(vinyl alcohol) (PVA) [19]. The different weight compositions of HA and PVA were tested. In order to show the electro-responsivity, the hydrogels were exposed to an electric field of 5V. The effect of on-off switching of the input voltage on the hydrogels is shown in Figure 2.16. When the electric field was applied, the hydrogels exhibited shrinking; when the electric field was switched off, the hydrogels expanded. This behavior was due to the migration of the positively charged

27

counter-ion in the hydrogel toward the cathode. This led to partial shielding of the carboxylate groups in HA, therefore reducing the extent of hydration of the hydrogel.
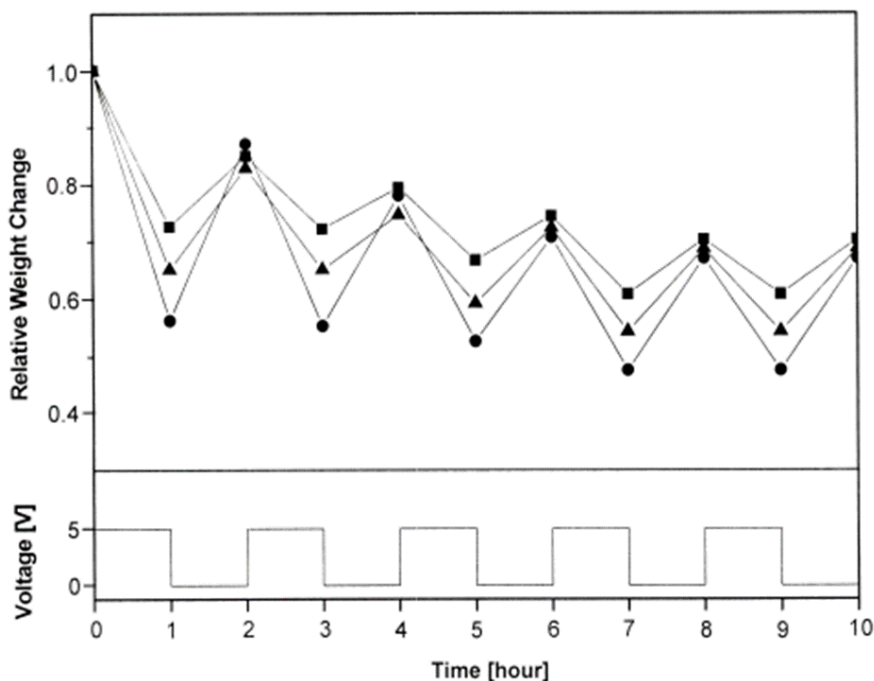
Figure 2.16. The Electro-responsiveness of HA/PVA hydrogels due to on–off switching of electric field (5 V) [19].

The response of the PEC hydrogels to an electric field can take a shape of eroding the polymeric network. It was reported that the insoluble PEC hydrogel (poly(allylamine) and heparin), became soluble by applying an electric field [15]. The PEC was attached to a platinum cathode in a continuously stirred buffer solution (pH 7.4), and an electric current of 10, 15, or 20 mA was applied in an on-off switching manner. Once the electric current was applied, a disintegration of the PEC matrix occurred due to the disruption in the ionic bond between heparin and poly(allylamine). This disruption resulted from the change in the pH around the cathode and the anode that led to deprotonation of the amine groups in poly(allylamine) and neutralization of acidic groups in heparin. The disintegration in the PEC network allowed the heparin to be released. As the electric current increased, the release of the heparin increased as shown in Figure 2.17.

28
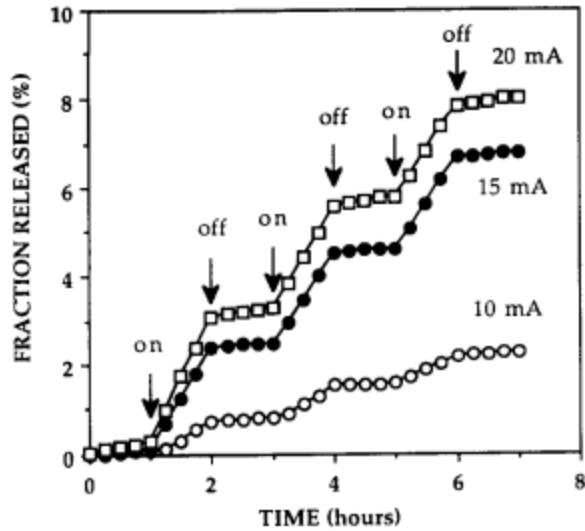
Figure 2.17. The release of heparin from poly(allylamine) /heparin PEC in PBS with the application of different electric currents [15].

Another PEC hydrogel, one that was composed of silk fibroin and hyaluronic acid, was studied [85]. Passive release and active release under a current density of 0.5 mA/cm^2 were performed using timolol maleate salt (TM) as a model drug because it is trans-dermally well tolerated in humans. The results indicated that the drug permeation through PEC hydrogel was enhanced under an electric field. In contrast, the loaded membranes did not respond to the electric field due to the strong interactions between the drug and the PEC matrix (Figure 2.18).
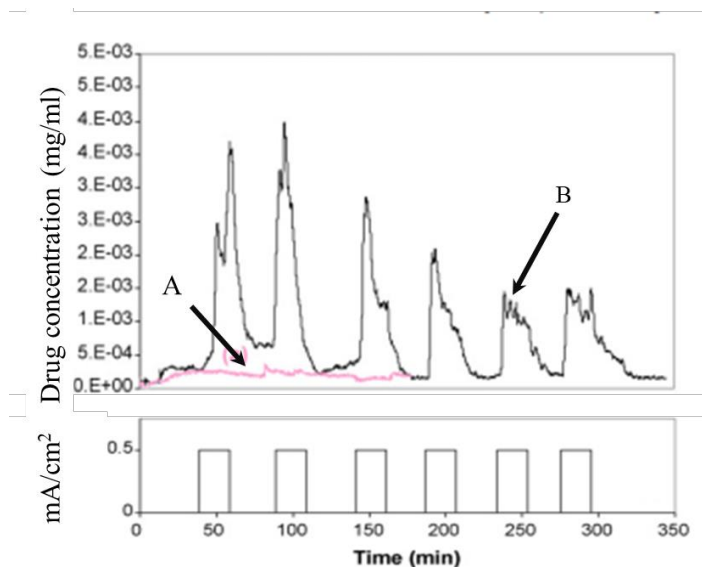
Figure 2.18. TM delivery profiles through silk fibroin/hyaluronic acid PEC. (A) TM permeation through the membrane in passive mode. (B) electro-responsive permeation [85].

2.3.3.4 Active release: Light

Light-responsive PEC hydrogels provided on-demand drug release, even on the nanoscale. The triggered release of encapsulated cargo from light-responsive polyelectrolyte nanocomplexes was achieved [17]. The polyelectrolyte nanocomplex that composed of anionic poly(styrene sulfonate) (PSS) and a charge-shifting polycation (P1, that was obtained via the copolymerization with the hydrophilic neutral monomer oligo(ethylene glycol) methacrylate). Nile Red was used in this study as a model drug. When the ultraviolet light was applied, photolysis of nitrobenzyl groups occurred that changed P1 into polyanion P− (see Figure 2.19 (A)). The distribution of the ion-pairing between P− and PSS led to dissolve the polyelectrolyte nanocomplex and then the controlled release of the encapsulated Nile Red. (see Figure 2.19 (B))
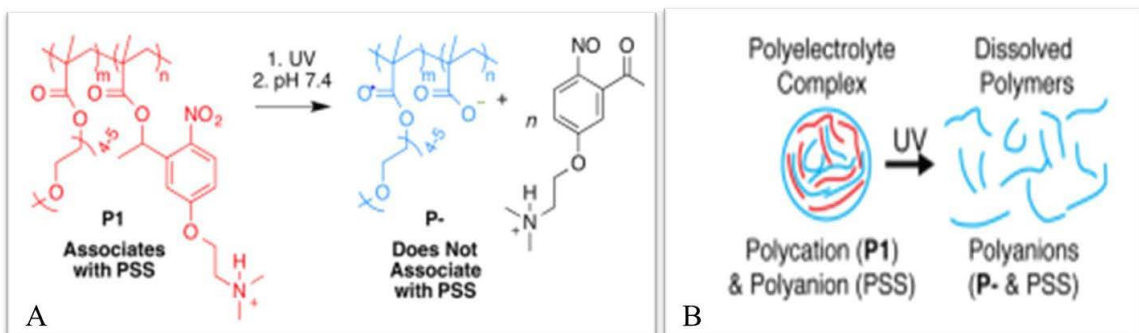
Figure 2.19. (A) Photoinduced charge-shifting of positively charged P1 to negatively charged P−. (B) Schematic of the light-triggered disruption of PECs [17].

2.3.3.5 Active release: Temperature

Thermo-responsive PEC hydrogels can be obtained by incorporating thermo-responsive polymers that undergo reversible phases with the temperature change. When the temperature increases to higher than the polymer's lower critical solution temperature (LCST), the polymer enters the one-phase region, therefore a higher drug release occurs. A thermo-responsive hydrogel composed of ALG beads containing poly(N-isopropylacrylamide) (PNI-PAAM) and coated with CHI was obtained [86]. The coating was done based on the interaction of amine groups in CHI and carboxylate groups in ALG. The LCST was found to be 31°C for this case. The indomethacin drug release profiles of the hydrogels as a function of temperature were investigated. At 37°C, the PEC samples showed a higher drug release rate, and a lower drug release rate was obtained at 25°C. It was explained that the higher release rate at 37°C resulted from the precipitation of PNIPAAM above LCST, which led to squeezing the drug out. As a disadvantage of this work, the hydrogel may provide the drug at a higher rate at a normal skin temperature (noninfected), since the LCST of the hydrogel is close to the normal body temperature (38°C). The LCST needs to be adjusted to provide the drug at a proper time when the skin temperature exceeds the normal range.

Another study reported thermo-responsive PEC hydrogel composed of chitosan-g-N-isopropylacrylamide (PNIPAM) and pectin that exhibited swelling under a temperature of 33.1°C (which is the LCST of NIPAM), and sharp shrinking at lower temperatures [87]. A different thermo-responsive polymer was used to obtain thermo-

31

responsive PEC hydrogel in a study conducted [16]. Polyalkyleneoxide–maleic acid (PAOMA) is an anionic polymer that can have various LCST, depending on the change of alkyleneoxide (AO) chain composition. The PEC obtained was composed of CHI and PAOMA. Salicylic acid was used as a model drug for this work. The drug release behavior was tested at 25°C and 50°C. The results indicated that an increase in the release rate was observed at 50°C, while a decrease in the release rate took place at 25 °C. This could be explained by the changes that occurred to the hydrophobic AO chain in POMA. Above LCST, it tends to form a micelle-like structure as shown in Figure 2.20. As a result of the structural changes in POMA chains, a repulsion force occurred between the carboxylate groups in POMA the anionic drug. Therefore, an increased release rate was observed. The advantage of creating this hydrogel is that the LCST could be adjustable compared to the previously mentioned studies [86] [87]. Because PAOMA has been used in the structure, it can change the swelling behavior of the hydrogel by having different LCST and by changing the composition of the AO chain.
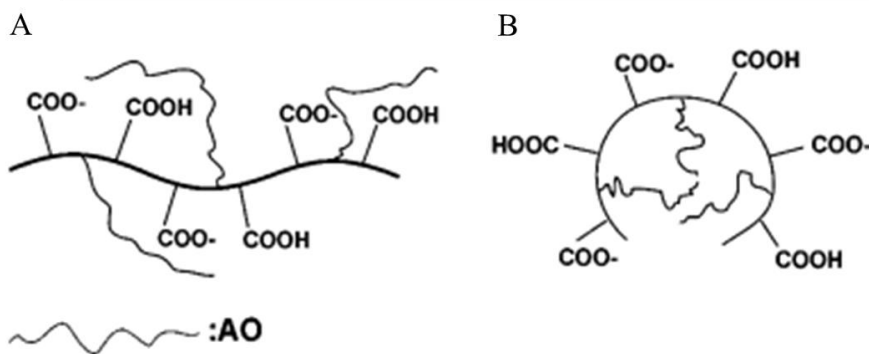
Figure 2.20. hydrophobic PAOMA molecule at (a) 25 °C and (b) 50 °C [16].

Table 2.3. Comparison of the responsive PEC hydrogels.

PEC composition	Response type	Response shape	Drug/model drug/incubation	Reference
poly(2-(dimthylamino) ethyl methacrylate) and poly (acrylic acid)	pH	Swelling and shrinking	HCl and NaOH	[84]
CHI and Xanthan	pH	Swelling and shrinking	HCl and NaOH	[18]
hyaluronic acid (HA) and poly(vinyl alcohol) (PVA)	Electrical	Shrinking	Water	[19]
poly(allylamine) and heparin	Electrical	Eroding	Heparin	[15]
silk fibroin and hyaluronic acid	Electrical	Swelling	Timolol maleate salt	[85]
poly(styrene sulfonate) and a charge-shifting polycation	Light	Eroding	Nile Red	[17]
alginate beads containing poly(N-isopropylacrylamide) (PNI-PAAM) and coated with chitosan	Temperature	Swelling and shrinking	Indomethacin	[86]
CHI and Polyalkyleneoxide–maleic acid	Temperature	Swelling and shrinking	Salicylic acid	[16]

chitosan-g-N-isopropylacrylamide and pectin	Temperature	Swelling and shrinking	Coomassie Blue	[87]

3. Methodology

Chemically and electrically regulated Fc-CHI/ALG PEC hydrogel was obtained and characterized. This chapter presents the methods and tests that were performed to characterize CHI/ALG PEC hydrogel as a control, as well as the conjugated version of Fc-CHI/ALG PEC hydrogel.

3.1. Materials

Low molecular weight chitosan and alginic acid sodium salt from brown algae (medium viscosity) were purchased from Sigma–Aldrich. Ferrocenecarboxaldehyde, 97% and Sodium cyanoborohydride 95% were obtained from Alfa Aesar. Fluorescein isothiocyanate-dextran (average Mw 3000-5000 Da) was purchased from Sigma–Aldrich. Fluorescein, pure (Mw = 332 g/mol) was obtained from Sigma–Aldrich. Agarose LE was obtained from BioExcell.

3.2. Synthesis of ferrocene conjugated chitosan

Three different amounts of Fc were used in the synthesis of Fc-CHI (low, medium, and high) according to previous work [26, 87]. The Fc amounts were adjusted to keep freely available amine groups interacting with the ALG for PEC formation. The Fc-CHI was synthesized as follows. CHI (0.9 g) was dissolved in 0.1 M acidic acid solution (360 mL deionized water, 2.058 mL acetic acid, pH=3) using a magnetic stirrer with a stirring time of 24 hours. Ferrocene carboxaldehyde (3.1, 4.7, and 9.1 mg for low, medium, and high amounts of Fc, respectively) was dissolved in 340 mL of methanol and then added to the first solution (while stirring), after stirring the solution (550 rpm) for 1 hour at room temperature. Sodium cyanoborohydride (1.8, 2.7, and 5.4 mg for low, medium, and high amounts of Fc, respectively) was dissolved in 20 ml of methanol and then added dropwise to the mixture. After 24 hours of mixing on the magnetic stirrer at 550 rpm, 23 mL of 5 % sodium hydroxide was added dropwise to the mixture until precipitates formed. The products were separated by filtration and washed eight times, the first two times using 70 % methanol, the second two times using 80 % methanol, and

then two times with 90 % methanol, and the last two using pure methanol. The volume used for each wash was 150 mL. Finally, the products were dried overnight through evaporation, and then they were ready to be used for other experiments (Figure 3.1)
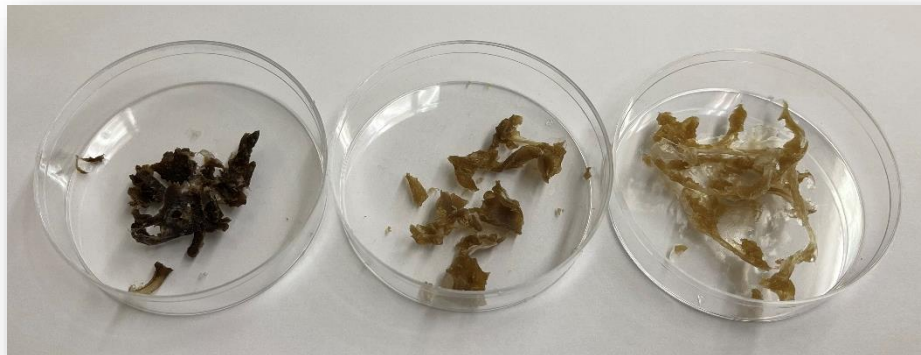
Figure 3.1. Dry Fc-CHI products. High, medium, and low amounts of Fc (from left to right)

3.3. PEC preparation

3.3.1. CHI/ALG PEC preparation

ALG solution (2 % w/v) was prepared by dissolving 0.4 g of ALG powder in 20 mL of deionized (DI) water. The solution was stirred for 24 hours at 500 rpm and at room temperature. CHI solution (2 % w/v) was prepared by dissolving 0.4 g of CHI powder in 20 mL of deionized water containing 100 μL acetic acid (0.5 % by weight). The solution was stirred for 24 hours. In order to form the PEC, 16 mL of ALG solution was added slowly to 4 mL of CHI solution (20 % CHI, 80 % ALG) while stirring. The solution was stirred for 40 minutes at 200 rpm. The solution was centrifuged at 6000 rpm for 8 minutes to remove the captured bubbles and then poured into a petri-dish with a diameter of 3 cm. After that, the sample was placed in a HCUCFS-404 freezer (VWR, Pennsylvania, USA) at -20 °C for 24 hours then lyophilized at -50 °C in the freeze dryer to form the PEC hydrogel dried (Figure 3.2).

36

Figure 3.2. Image of Labconco freeze dryer.

3.3.2. Fc-CHI/ALG PEC preparation

In order to prepare Fc-CHI/ALG PEC, a similar procedure to CHI/ALG PEC preparation was used. Fc-CHI solution (2 % w/v) was prepared by dissolving 0.4 g of Fc-CHI powder in 20 mL of DI water containing 100 µL acetic acid (0.5 % by weight). The solution was stirred for 24 hours. ALG solution (2 % w/v) was prepared as mentioned previously in section 3.2.1 Fifteen mL of ALG solution was added slowly to 5 mL of CHI solution (25 % CHI, 75 % ALG) while stirring. The solution was stirred for 40 minutes at 200 rpm and then centrifuged, frozen and lyophilized as mentioned in section 3.2.1.
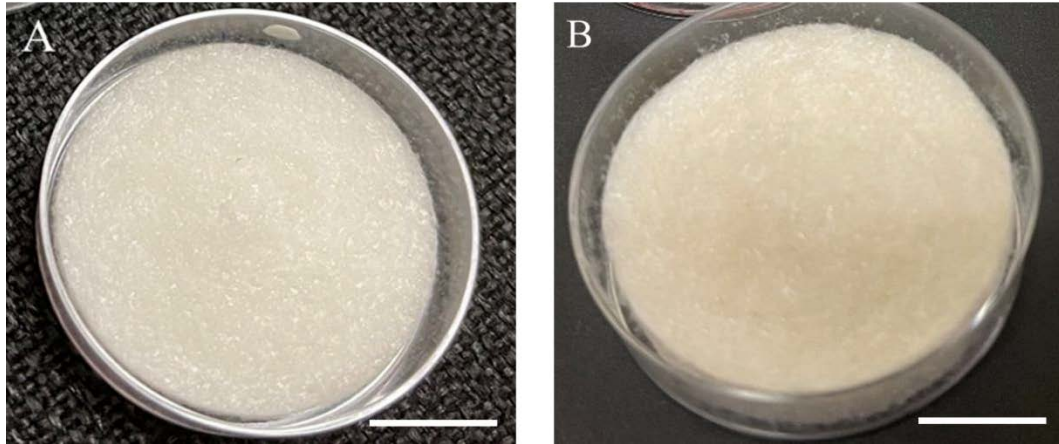
Figure 3.3. Images of (A) dry CHI/ALG PEC and (B) dry Fc-CHI/ALG PEC. (Scale bar 1cm)

3.4. Characterizations

The PEC hydrogels were characterized by turbidity measurements, Attenuated Total Reflectance Fourier Transform Infrared Spectroscopy (ATR-FTIR), scanning electron microscopy (SEM), swelling behavior test, and gel content tests.

3.4.1. Turbidity test

The turbidity measurements of the PEC hydrogels were taken to find the optimum ratio between ALG, and CHI or Fc-CHI [76]. A Thermo Scientific Orion AQ4500 turbidity meter (Thermo Scientific, Beverly, USA) was used for this purpose (Figure 3.4). The turbidity meter works by sending a light beam into the solution to be tested. The results were presented in a nephelometric turbidity unit (NTU). The concentrations 0.5, 1.0, 1.5, and 2.0 % (w/v) of CHI and ALG solutions were used to prepare different ratios of CHI/ALG PEC hydrogels. Four ratios of CHI and ALG solutions were prepared of each concentration for this test, (20 % CHI, 80 % ALG), (40 % CHI, 60 % ALG), (60 % CHI, 40 % ALG) and (80 % CHI, 20 % ALG). All the samples were centrifuged in order to remove the captured bubbles because the bubbles affect the turbidity reading due to the change in the reflection of the light in the turbidity meter. After that, the samples were transferred to the turbidity meter's vials, and the readings were taken.

The turbidity measurements also were taken for Fc-CHI/ALG PEC hydrogels. 2 % (w/v) solutions of ALG and the three different amounts of Fc-CHI (low, medium, and high) were used to prepare different ratios of Fc-CHI/ALG PEC hydrogels. Turbidity tests were performed on these samples as well.

Figure 3.4. Thermo Scientific Orion AQ4500 turbidity meter

3.4.2. ATR-FTIR analysis

The ATR-FTIR spectra of CHI, ALG, CHI/ALG PEC, Fc, Fc-CHI (three different concentrations of Fc), and Fc-CHI/ALG PEC were registered by a PerkinElmer Spectrum Two FTIR spectrometer with universal ATR accessory (PerkinElmer, Waltham, USA) as shown in Figure 3.5. The spectra were recorded for the dry samples between 450 and 4000 cm^{-1} by 16 scans and it was taken 3 times for each sample, in order to detect the characteristics band of the materials, as well as to confirm PEC formation.

Figure 3.5. PerkinElmer ATR-FTIR

3.4.3. SEM imaging and EDS

The morphologies of CHI, Fc-CHI, ALG, CHI/ALG PEC, Fc-CHI/ALG PEC were analyzed using (KEYSIGHT, Santa Rosa, USA) SEM with an accelerating voltage of 2 kV. Because the samples are nonconductive, they were coated with a thin layer of gold-palladium using Polaron sputter coater E5100 (Polaron, Laughton, UK) under a vacuum of 0.1 torr and current of 20 mA, for 3 minutes. Also, energy dispersive X-ray spectrometer (EDS) analysis was carried out for CHI and Fc-CHI samples, in order to prove that the Fc-CHI sample exists Fc in the composition.

3.4.4. Swelling behavior

The swelling behavior of CHI/ALG and Fc-CHI/ALG PEC hydrogels was determined by incubating the dry samples (size 0.5 cm^3) at room temperature in phosphate buffer saline (PBS, 10 mM, pH 7.4). At first, the weight of each dry sample was measured, and then each sample was placed in 1 mL of PBS for 24 hours. After that, the wet samples were removed from the media and placed on a filter paper for 10 seconds to remove the adsorbed PBS on the surface, then weighted on the lab scale. The swelling percentage was calculated using the following equation.

$$E_{sw} = \frac{W_{wet} - W_{dry}}{W_{dry}} \times 100$$ **Equation 3-1**

Where E_{sw} is the swelling percentage, W_{wet} is the weight of the wet sample, and W_{dry} is the weight of the dry sample. For this experiment, three samples of each PEC hydrogel were tested, and the average of the results was found.

3.4.5. Gel content

In order to prove the stability of the CHI/ALG and Fc-CHI/ALG PEC hydrogels, the gel content test was performed. Three dry samples of each PEC hydrogel that had a size of 0.5 cm^3 were weighed and then immersed in PBS for 24 hours. The wet samples were removed from the incubation media and then placed in the freezer (-20 °C) for 24 hours. After that, the samples were lyophilized at -50 °C in the freeze dryer. The weight of the freeze-dried samples was measured and then used in Equation 3-2 to find the gel content percentage.

$$Gel(\%) = \frac{W_d}{W_i} \times 100 \hspace{4cm} \textbf{Equation 3-2}$$

Where Gel (%) is the gel content percentage, W_d is the weight of freeze-dried samples, and W_i is the initial weight of the samples. The average of the results was found as the percentage of the gel content.

3.5. Drug release studies

3.5.1. Drug release in solution

In order to study the drug release behavior of CHI/ALG and Fc-CHI/ALG PEC hydrogels, Fluorescein-dextran (FITC-D) and fluorescein (FITC) were used as model drugs. FITC-D and FITC were dissolved in PBS at a concentration of 0.005 mg/mL. The dry PEC samples were incubated in the model drug solutions for 48 hours. After that, the samples were rinsed two times each, by placing them in 1mL of fresh PBS solution for 1 minute for each rinse. The samples were then transferred to microcentrifuge tubes containing 1 mL of PBS solution. The tubes were covered with aluminum foil due to the sensitivity of the FITC-D and FITC to light and placed at room temperature. Then, 0.5 mL of the incubation media was withdrawn and replaced with the same volume of fresh

PBS solution at determined time intervals over 72 hours. During this time the withdrawn samples were labeled and stored in the refrigerator. The released amount of FITC-D and FITC was determined using a BioTek Cytation 1 spectrophotometer (BioTek, Winooski, USA) shown in Figure 3.6. The incubation solutions, the rinsing solutions, and the withdrawn samples were transferred to a 96-well plate (200 µl in each well) and then the intensity of the FITC-D and FITC were measured using the spectrophotometer. Fluorescence (excitation and emission wavelengths of 485 and 528 nm) and absorbance modes (absorbance at 490 nm) were used in the spectrophotometer for FITC-D and FITC solutions, respectively. In order to convert the intensity to concentration, a calibration curve was created by doing a serial dilution for FITC-D and FITC solutions that have a concentration of 0.005 mg/mL, and the intensity of the diluted solutions was measured using the spectrophotometer. The intensity values were plotted versus the concentrations and then the curve equation was found and used to convert the intensity to concentration. To calculate the amount of the incubated drug and the percentage of the released drug at a specific time, the intensity readings were converted to concentration and then the following equations were used:

Drug incubated in the PEC hydrogel = Original concentration (0.005 mg/mL) − (The concentration of incubation solution + The concentration of rinsing solutions)
Equation 3-3

Drug released at a specific time (e.g., after 1 hour) = Drug incubated in the PEC hydrogel − The concentration of the solution at this time (1 hour)
Equation 3-4

Percentage of drug released at a specific time (e.g., after 1 hour) = (Drug released at 1 hour/ Drug incubated in the PEC hydrogel) ×100
Equation 3-5

The percentage of the drug released was found at each of the times of withdrawing the samples over the 72 hours and then plotted versus the time to show the drug release

42

behavior of the samples. (Three samples were used of each hydrogel for this experiment and the average was found.)

Figure 3.6. BioTek Cytation 1 cell imaging multi-mode reader

3.5.2. Drug release on agarose gel (Passive)

In order to study the drug release on agarose gel (acting for research purposes as a phantom skin), the experiment was designed as follows. A polydimethylsiloxane (PDMS) sheet was created by mixing 20 mL of elastomer base with 2 mL of curing agent (10:1 mixing ratio) for 5 minutes and then poured into a petri-dish (diameter = 10 cm). The captured bubbles were removed by placing the petri-dish in a vacuum pump with the pressure gauge reading between -20 to -23 bar, for 30 minutes. Afterward, the sample was placed in the oven at 80 °C for 2 hours to obtain an elastic PDMS sheet. The thickness of the resulted PDMS sheet yielded about 0.5 cm. The sheet was used to prepare a mold to hold the agarose gel, as shown in Figure 3.7 (A). The agarose gel was prepared by dissolving 0.6 g of agarose powder in 30 mL of PBS solution and then microwaved for

43

4 minutes in order to have a fully homogenous solution. Using a micropipette, the liquid agarose solution was poured into the PDMS mold to create an agarose gel layer, the agarose solution was allowed to leak under one side of the mold to create an attached thin layer of agarose gel that will be used as a base to the PEC hydrogels, to prevent the leakage of the drug released under the layer that acts as phantom skin. The agarose solution was left for 2 minutes to cool and solidify. It was then ready for use in the experiment (Figure 3.7 (B))

The passive release behavior of CHI/ALG and Fc-CHI/ALG PEC hydrogels was studied using FITC-D and FITC as model drugs. FITC-D and FITC solutions were prepared in a concentration of 0.005 mg/mL in PBS solution. The PEC samples were prepared in size of (1 cm × 0.5 cm × 0.5 cm) and then immersed in the model drug solutions for 48 hours. Afterward, the samples were taken from the incubation media and rinsed for 1 minute twice using fresh PBS solution. Then the samples were placed on a filtration paper for 10 seconds to remove the excess solution on the surface. After that, each sample was carefully placed attached to the prepared agarose gel as shown in Figure 3.7 (C). The whole assembly was then transferred to Zeiss Axio Vert A1 inverted microscope (Zeiss, Oberkochen, Germany) in order to image the movement of the model drugs through the agarose gel (see Figure 3.7 (D)). An image was taken every 10 seconds. The fluorescence mode was carried out with a FITC channel, a LED light intensity (30 %), an exposure time (500 ms), and a 20x objective lens. The middle of the agarose gel layer was focused during the time-lapse imaging.
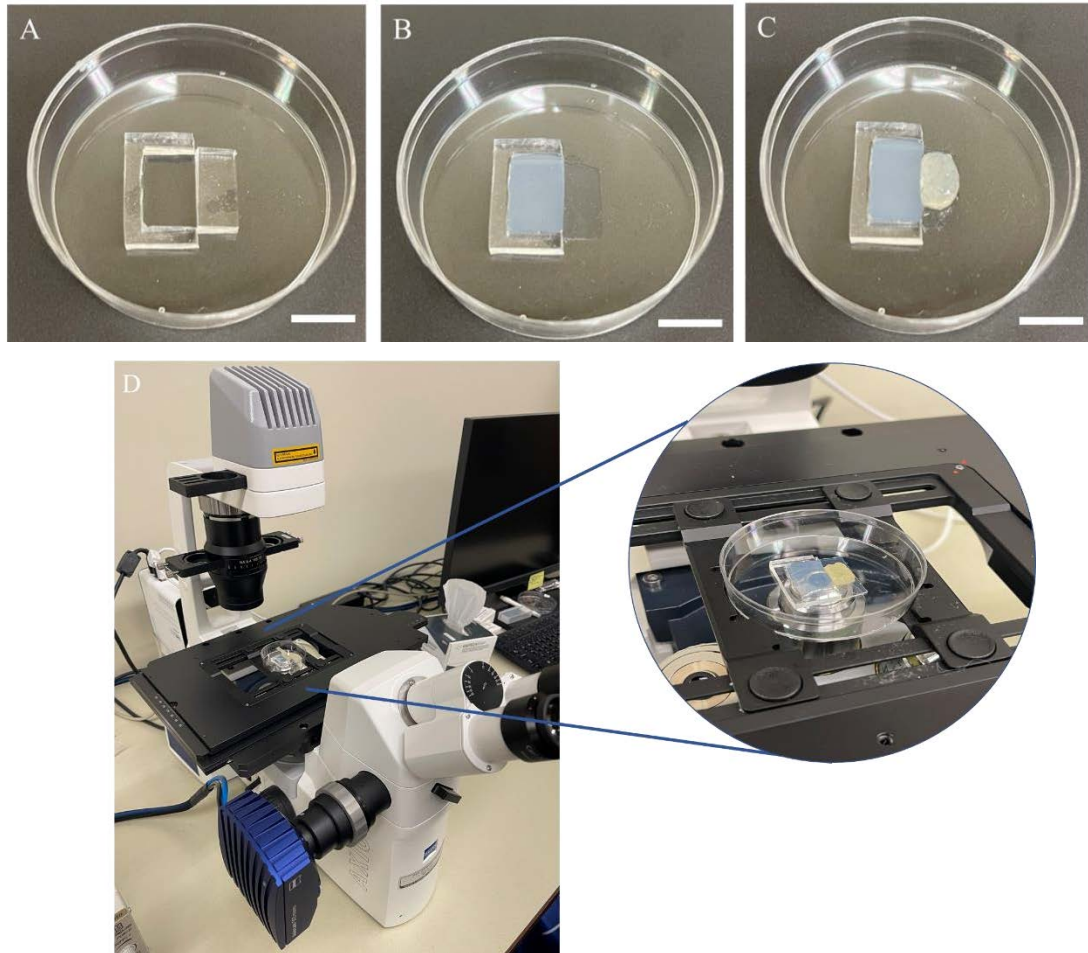
Figure 3.7. (A) The prepared PDMS mold. (B) Agarose gel layer (thickness = 0.5 cm), attached to thin layer created as a base to the loaded PEC hydrogel. (C) Loaded PEC hydrogel was placed attached to the agarose gel layer in order to test the passive release of the model drugs. (D) Image of Zeiss Axio Vert A1 inverted microscope during the time-lapse imaging. (Scale bar 1cm)

3.5.3. Drug release on agarose gel (Active)

In order to study the active release of the PEC hydrogels, a voltage was applied to demonstrate the effect of the electric field on the release behavior. The same experiment design with the same conditions as explained for the passive release was used for the active release. The only difference was the addition of two platinum (Pt) wires as electrodes that were fixed on the Petri dish lid (the petri dish that held the agarose gel

layers inside) by creating a slit in the lid and fixing the wires (4mm apart) using PDMS blocks as shown in Figure 3.8(A) and (B). The Pt wires were connected to a power supply (Figure 3.8 (C)), the cathode electrode was inserted into the PEC hydrogel sample in the front (in a contact with the phantom skin), and the anode in the back.

Two voltage values (0.25 and 1 V) were applied to stimulate the PEC hydrogels, and the movement of FITC and FITC-D through the agarose gel overtime was imaged as explained in Section 3.4.2.
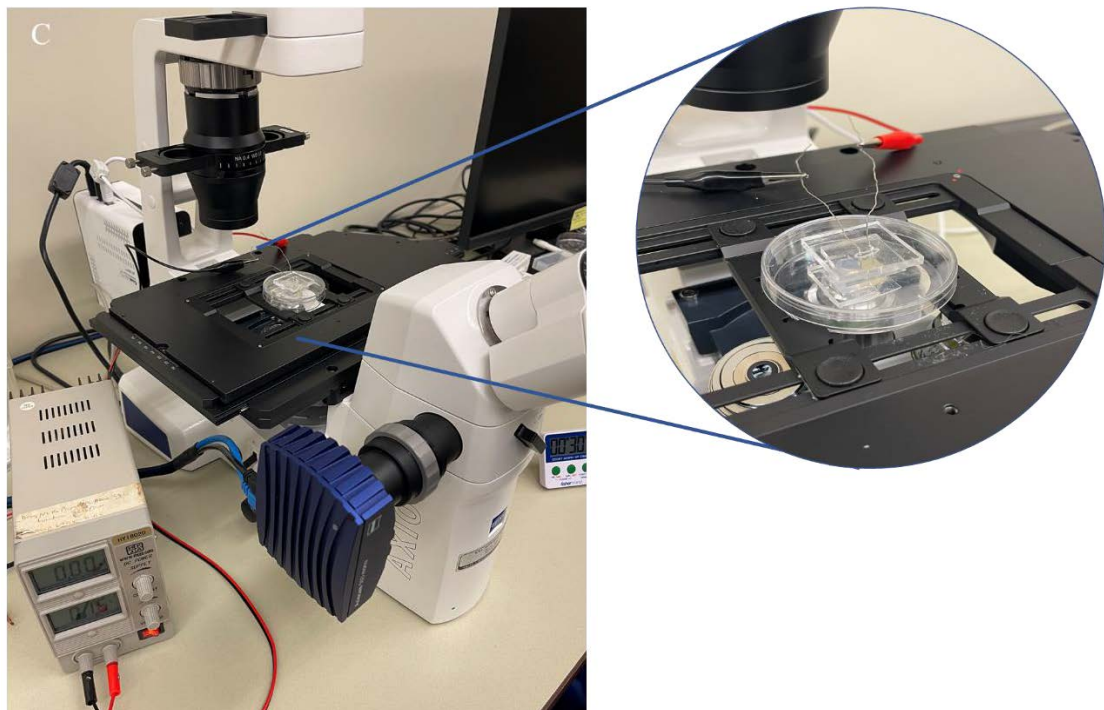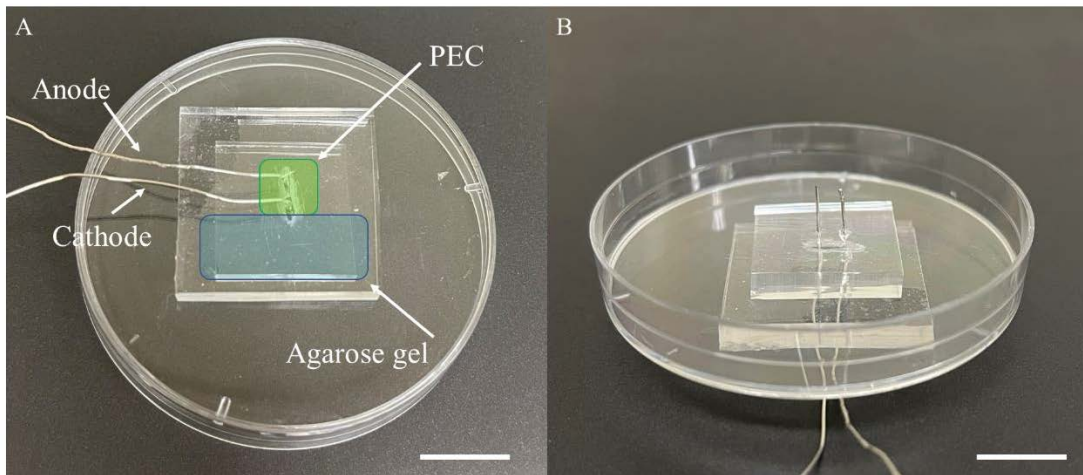
Figure 3.8. The design of the active release experiment; custom-made setup of two PDMS blocks holding the Pt wires through the lid (A) top view, (B) bottom view, and(C) the power supply device connected to the Pt wires that were inserted inside the PEC hydrogel during the time-lapse imaging. (Scale bar 1cm)

3.6. Diffusion coefficient calculations

The diffusion coefficient of the model drugs through the agarose gel can be estimated by fitting the intensity profiles of the FITC-D and FITC that were produced during the imaging using the microscope with an appropriate model based on the solution of Fick's second law [88, 89]. (Equation 3-5)

$$\frac{\partial c(x,t)}{\partial t} = D \frac{\partial^2 c(x,t)}{\partial x^2}$$ **Equation 3-5**

Where c is the concentration, x is the distance, t is the time, and D is the diffusion coefficient.

Equation 3-5 represents Fick's second law at various initial and boundary conditions, the boundary conditions in our experiment were:

1- $C = 0$, $t \to 0$, $x > 0$
2- $C \to \infty$, $t \to 0$, $x = 0$

The solution of Equation 3-5 led to Equation 3-6

$$\frac{C(x,t)}{C_0} = \frac{1}{2\sqrt{\pi D t}} exp\left(\frac{-x^2}{4Dt}\right)$$ **Equation 3-6**

Equation 3-6 was applied to experimental data in the form of Equation 3-7

$$I(x,t) = P_1 exp(-P_2 x^2)$$ **Equation 3-7**

where I is the intensity of FITC-D and FITC in arbitrary units and P_1 and P_2 are the fitting parameters.

From Equations 3-6 and 3-7:

$$P_2 \;=\; \frac{1}{4Dt} \quad \text{and} \quad D = \frac{1}{4P_2 t}$$

In order to solve the equation and find the values of P_1 and P_2, a custom-built MATLAB code was written and run to find P_1 and P_2, followed by D.

4. Results and discussion

4.1. PEC preparation

CHI/ALG PEC hydrogel was successfully formed through the ionic interaction between the positively charged amino group of CHI and the negatively charged carboxylic ion group of ALG as shown in Figure 4.1 (A). Also, Fc-CHI/ALG PEC was successfully obtained through the ionic interaction between the freely available amino groups of CHI (that remained after the conjugation of Fc into CHI, covalently through a chemical reaction) and carboxylic groups of ALG (Figure 4.1 (B))
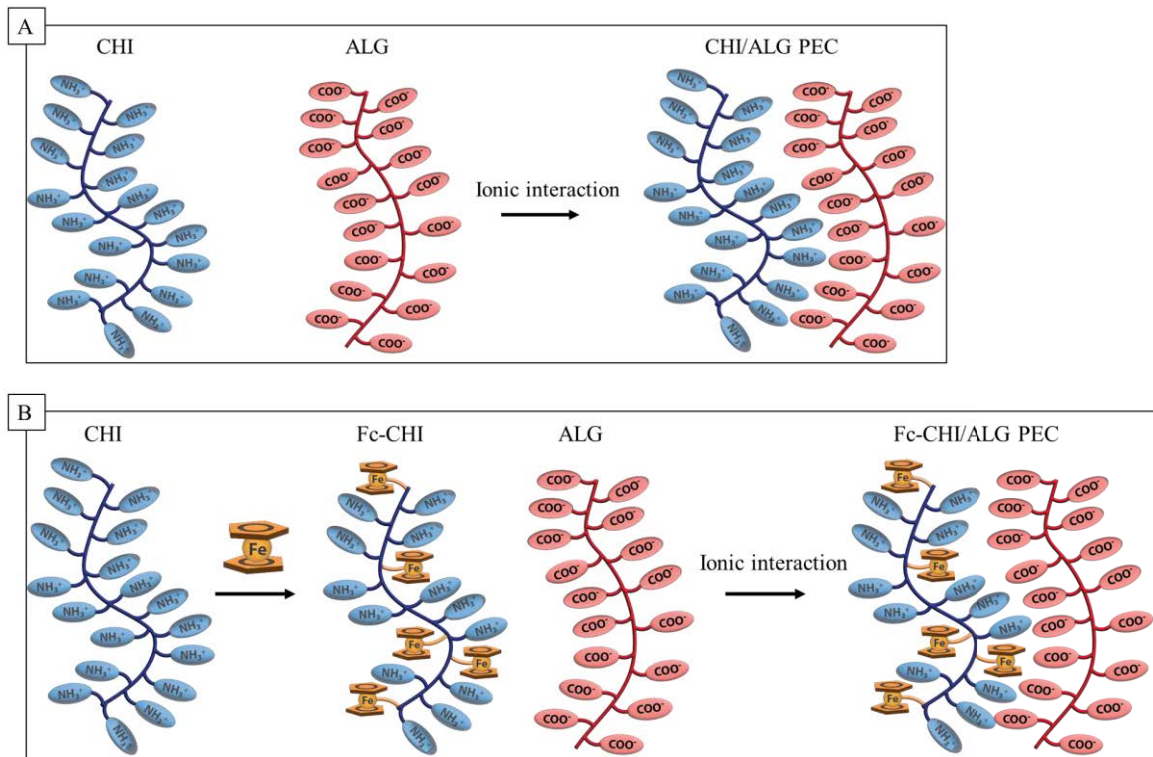
Figure 4.1. Schematic of the fabrication of CHI/ALG PEC (A), and Fc-CHI/ALG PEC (B).

4.2. Characterizations

4.2.1. Turbidity test

The aim of performing the turbidity test was to confirm the interaction between the CHI or Fc-CHI, and ALG, as well as to find the optimal ratio between the polyelectrolytes and the stoichiometric condition (1:1 of positively and negatively charged groups). For the CHI/ALG PEC, the highest turbidity values (NTU, Nephelometric Turbidity Unit) were noted for the ratio of (20% CHI, 80% ALG) to be 810, 640, 515, and 320 NTU for the concentrations 2, 1.5, 1, and 0.5%, respectively for both CHI and ALG solutions. The NTU values decreased with increasing the percentage of CHI and decreasing the percentage of ALG in the sample (Figure 4.2).

The highest NTU values can be considered as the points of charge-to-charge balanced PEC formation (1:1 stoichiometry), in which all positively charged amine groups of CHI were ionically bonded to negatively charged carboxylic groups of ALG, that may result in the precipitation of a largest amount of PEC, therefore more scattering of the turbidity meter's light [66-68, 90]. Figure 4.3 shows the visual gradient in the different NTU values of the prepared samples.

Moreover, the NTU values increased as the concentration of both CHI and ALG solutions increased. This can be explained by the increase in the density of the amine groups and carboxylic groups in the samples, therefore, precipitation of a larger amount of PEC.
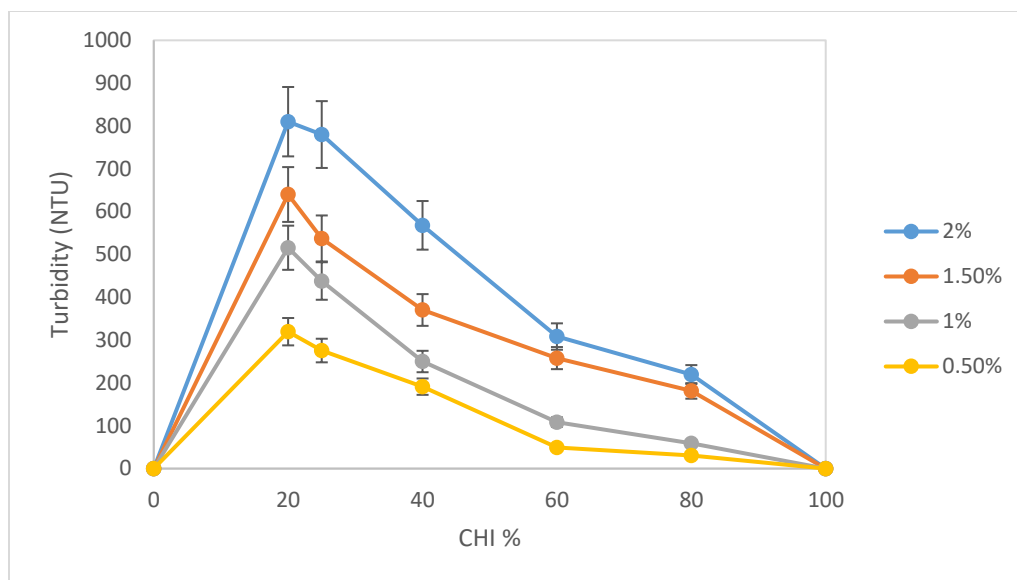
Figure 4.2. The turbidity curves for the CHI/ALG PEC hydrogels that were prepared with different concentrations of 0.5, 1.0, 1.5, and 2.0 % (w/v) of CHI and ALG, with respect to different ratios (n = 3).
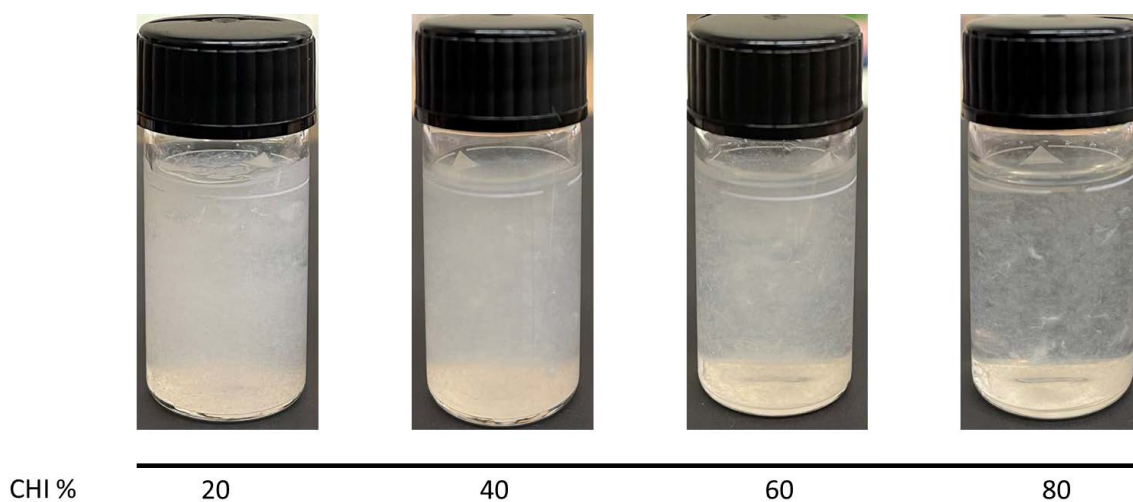
Figure 4.3. The gradient in the turbidity between the prepared samples of CHI/ALG PEC (2% (w/v))

The sample at the ratio of 20% CHI and 80% ALG and concentration of 2%(w/v) was selected as the optimized condition and characterized in terms of its mechanical stability and chemical functionality. Based on this control experiment, the Fc-CHI/ALG

PEC hydrogel samples (including the 3 amounts of Fc (low, medium, and high)) were examined to find out the stoichiometric condition. The maximum turbidities at the different ratios (20% Fc-CHI, 80% ALG; 25% Fc-CHI, 75% ALG; 40% Fc-CHI, 60% ALG) for low, medium, and high amounts of Fc, respectively, were found to be 870, 787, and 633, as shown in Figure 4.4.

The stoichiometric ratio between the samples that were prepared using a low amount of Fc was the same as the control sample (20% Fc-CHI,80% ALG). This can be explained by the availability of amine groups in Fc-CHI in a number that is close to the pure CHI, a result of conjugation of the small amount of Fc with free amine groups of CHI.

However, the stoichiometric ratio between the samples that were prepared using a medium amount of Fc shifted to (25% Fc-CHI,75% ALG). A higher percentage of Fc-CHI was needed at the stoichiometric ratio (25% Fc-CHI) due to less availability of amine groups in Fc-CHI compared to the control.

The peak shift of the high amount of Fc was larger than in other samples, resulting from the lower amount of the free amine groups in Fc-CHI.
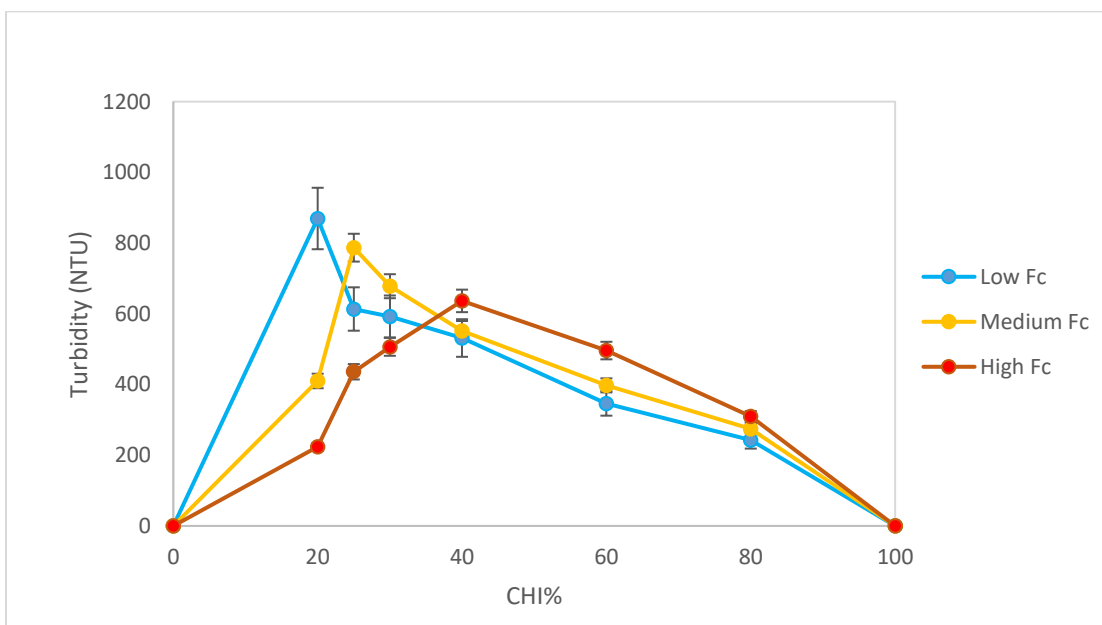
Figure 4.4. The turbidity curves of Fc-CHI/ALG PEC hydrogels that have low, medium, and high amounts of Fc conjugated in CHI.

4.2.2. ATR-FTIR analysis

CHI and Fc-CHI with different amounts of Fc (low, medium, and high) were analyzed using ATR-FTIR (Figure 4.5). The spectra of the samples showed a decrease in the absorbance of amide I ($\approx$1636 cm^{-1}) and amide II ($\approx$1542 cm^{-1}) peaks with an increase in the amount of Fc as follows, CHI > Fc-CHI(low Fc) > Fc-CHI(medium Fc) > Fc-CHI(high Fc), the results are shown in Table 4.1.

This decrease in the absorbance values between the samples confirms that there is less availability of amine groups of CHI as the amount of the reacted Fc increased, indicating that the Fc exists in the Fc-CHI in a higher concentration. The decrease in the absorbance of the amine group's characteristic peaks of Fc-CHI compared to pure CHI was observed in a study that synthesized Fc conjugated CHI. A new absorption band at about 814 cm^{-1} was detected in the spectrum of Fc-CHI indicating that the Fc has interacted with CHI [91]. Here in Figure 4.5, the peak was not detected due to the reduced amount of Fc that was used in the reaction.
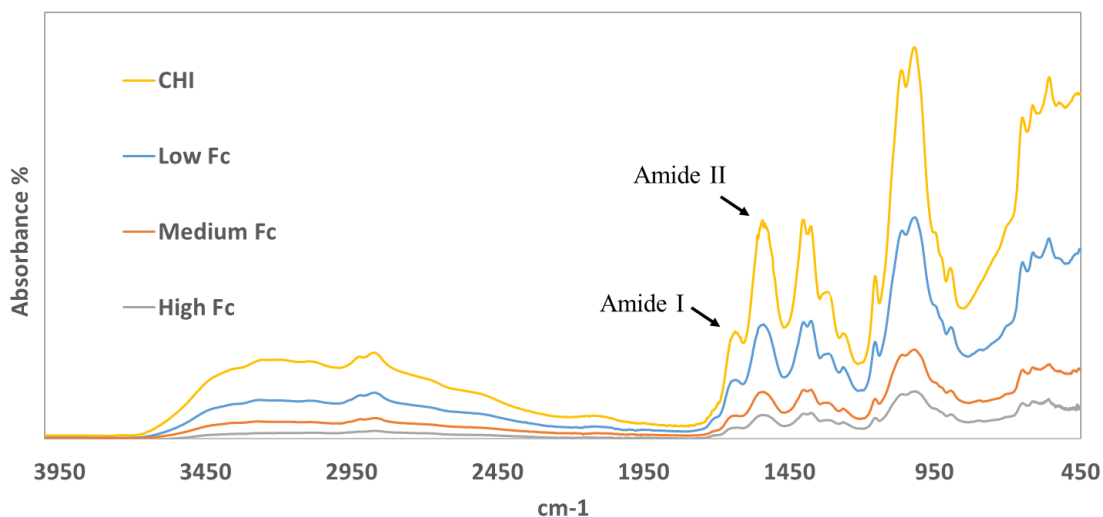
Figure 4.5. ATR-FTIR absorbance spectra of CHI, Fc-CHI (low Fc), Fc-CHI (medium Fc), and Fc-CHI (high Fc).

Table 4.1. The absorbance of amide I and amide II peaks of CHI, Fc-CHI (low Fc), Fc-CHI (medium Fc), and Fc-CHI (high Fc).

Sample	Amide I (cm^{-1})	Absorbance	Amide II (cm^{-1})	Absorbance
CHI	1636	0.075	1542	0.154
Low Fc-CHI	1634	0.041	1539	0.080
Medium Fc-CHI	1634	0.016	1538	0.033
High Fc-CHI	1634	0.008	1538	0.017

The ATR-FTIR analysis could also confirm the interaction between the polyelectrolytes by finding their characteristic peaks and observing the peak shifting. The spectra of ALG, CHI, Fc-CHI, CHI/ALG PEC, Fc-CHI/ALG PEC, and Fc are shown in Figure 4.6. The ALG spectrum showed the characteristic band of carbonyl (C=O) at 1593 and 1406 cm^{-1} that can be assigned to the asymmetric and symmetric stretching vibrations of carboxylate groups, respectively, and this is similar to observation from previous studies [92]. Characteristic absorption bands of CHI are usually observed between 1649 and 1652 cm^{-1} and 1558–1598, representing amide I and amide II groups, respectively [60]. These characteristic peaks were shifted to 1636 and 1541 cm^{-1} due to the effect of acetic acid (used to dissolve the CHI). The characteristic peaks of Fc-CHI shifted to 1634 and 1538 cm^{-1}, which indicated that CHI interacted with Fc. Disappearance of characteristic amide peaks of 1636 – 1541cm^{-1} of CHI and 1634 – 1538cm^{-1} of Fc-CHI in addition to peak shift of ALG characteristic band from1593 cm^{-1} to 1598 cm^{-1} (detected in CHI/ALG PEC as well as Fc-CHI/ALG PEC spectra), confirms PEC formation.

The intensity of the peak 1598 cm^{-1} in CHI/ALG PEC was higher, indicating that the degree of ionic interaction between the negatively charged carboxylic group of ALG and the positively charged amino group of CHI was stronger than that in Fc-CHI/ALG PEC, due to the absence of Fc. The characteristic peak of Fc was found at 1675 cm^{-1}, similar to observations in previous work [26].
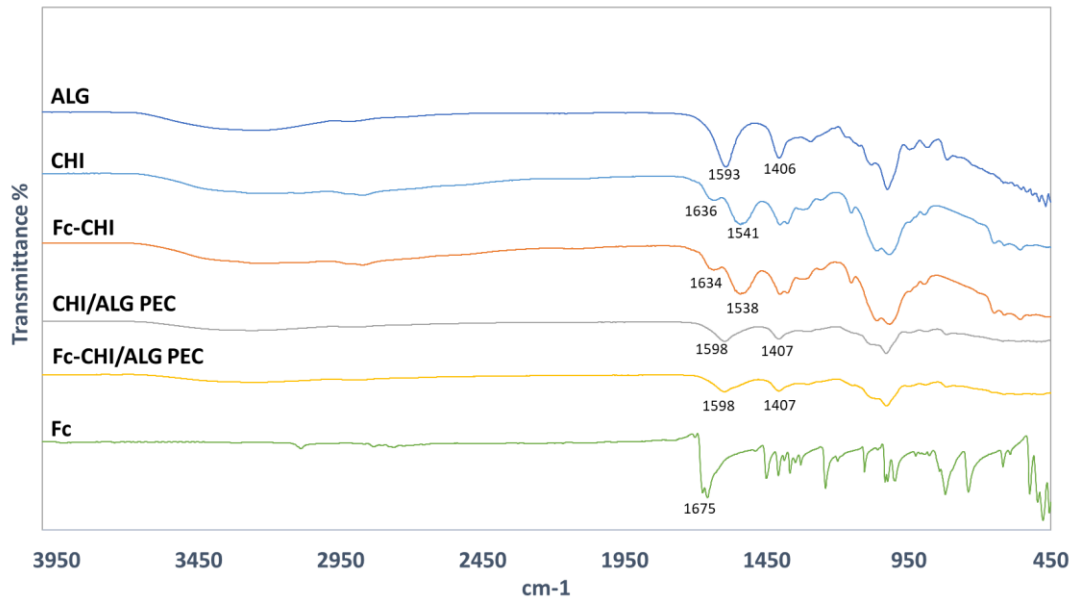
Figure 4.6. ATR-FTIR transmittance spectra of ALG, CHI, Fc-CHI, CHI/ALG PEC, Fc-CHI/ALG PEC, and Fc

4.2.3. SEM imaging and EDS

The morphologies of the ALG, CHI, Fc-CHI, CHI/ALG PEC, and Fc-CHI/ALG PEC samples are shown in Figure 4.7. Depending on the composition, there were differences in the appearance of the fibrillar structure of the samples. As shown in Figure 4.7(A) and (B), the pure ALG and CHI showed a relatively regular network due to the homogeneity of the samples. As shown in Figures 3.7 (B) and (C), CHI and Fc-CHI showed similar morphology. The porous structure of the PEC samples is shown in Figure 3.7 (D) and (E).
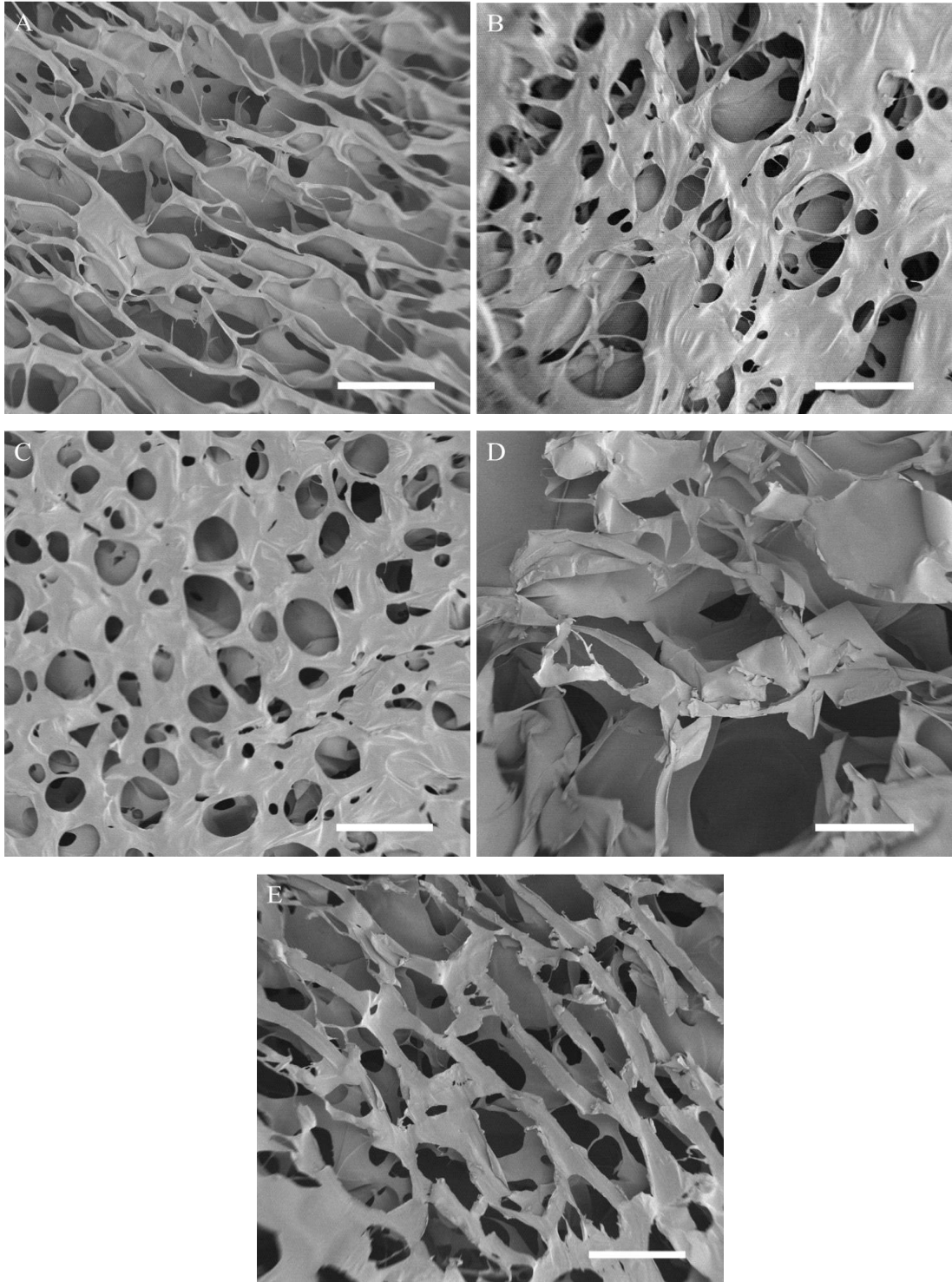
Figure 4.7. The morphologies of (A) ALG, (B) CHI, (C) Fc-CHI, (D) CHI/ALG PEC, and (E) Fc-CHI/ALG PEC. (Scale bar 50 μm)

Elemental compositions of CHI and Fc-CHI were analyzed using EDS during SEM measurements (Figure 4.8). In comparison with the CHI, there are a few additional peaks in the spectrum of Fc-CHI at 0.7 and 6.4 KeV, attributed to Fe sandwiched between two cyclopentadienyl rings in the staggered conformation of ferrocene, indicating that Fc was covalently conjugated with CHI. These observations were seen in a previous study [93].
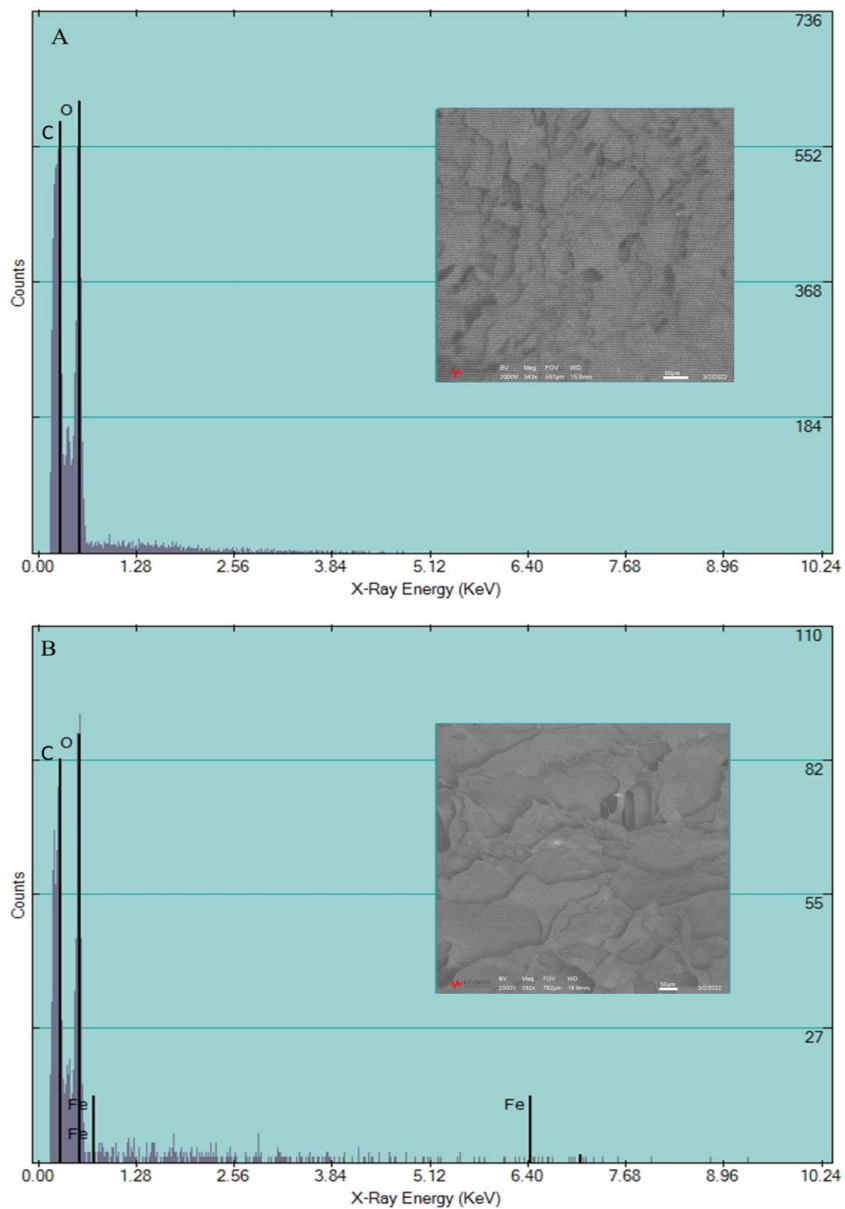
Figure 4.8. EDS analysis for (A) CHI, (B) Fc-CHI. The insets are SEM images (Scale bar 50μm).

4.2.4. Swelling behavior

The swelling ratios of CHI/ALG, Fc-CHI/ALG (low Fc), and Fc-CHI/ALG (medium Fc) PEC hydrogels were found to be 3480, 3692, and 4471%, respectively, as shown in Figure 4.9. These ratios are compatible with the previous study in preparation of CHI/ALG PEC as a drug delivery system for dermal wound healing, which reported that a stoichiometric PEC hydrogel had a swelling ratio of 3806% [64]. The increased water uptake of the PEC hydrogels with the increase of the Fc amount in the sample may be explained by the interaction of some of the amine groups of CHI with Fc and the ability of Fc-CHI chains to expand more and retain a larger amount of water within the porous structure.
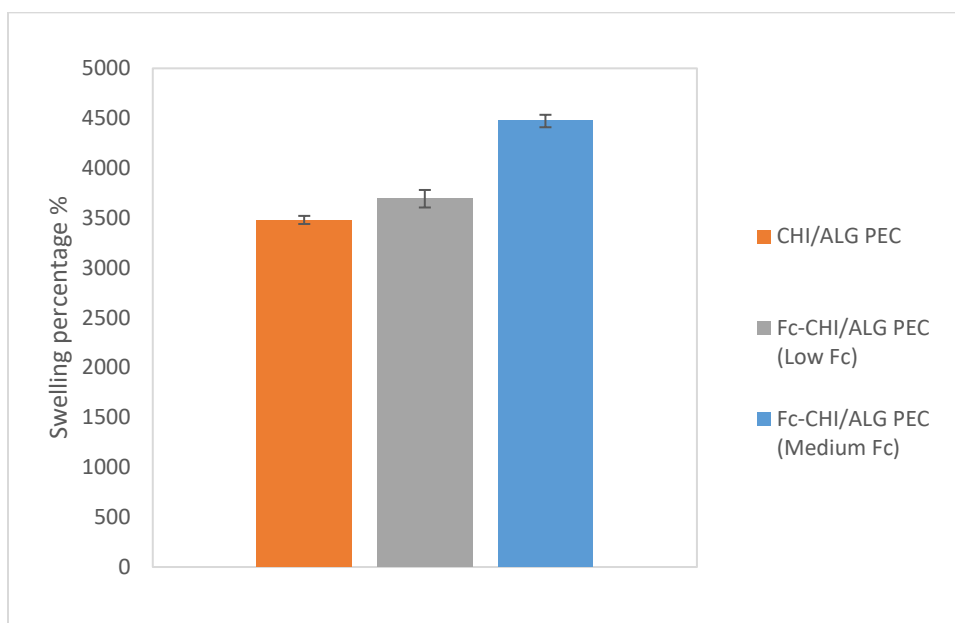
Figure 4.9. The swelling ratios of CHI/ALG, Fc-CHI/ALG (low Fc), and Fc-CHI/ALG (medium Fc) PEC hydrogels.

4.2.5. Gel content

It was found that all the PEC hydrogels showed almost 100% gel content (Figure 4.10), indicating that the PEC hydrogels were stable in the PBS solution and confirming that the interaction between CHI or Fc-CHI, and ALG was (1:1) stoichiometric, therefore, the hydrogels were insoluble in aqueous solution. Similar results were reported from a previous study that showed CHI/ALG PEC hydrogel films that also had a gel content percentage of 100%, confirming that the obtained PEC hydrogels were stable in aqueous solutions [92].
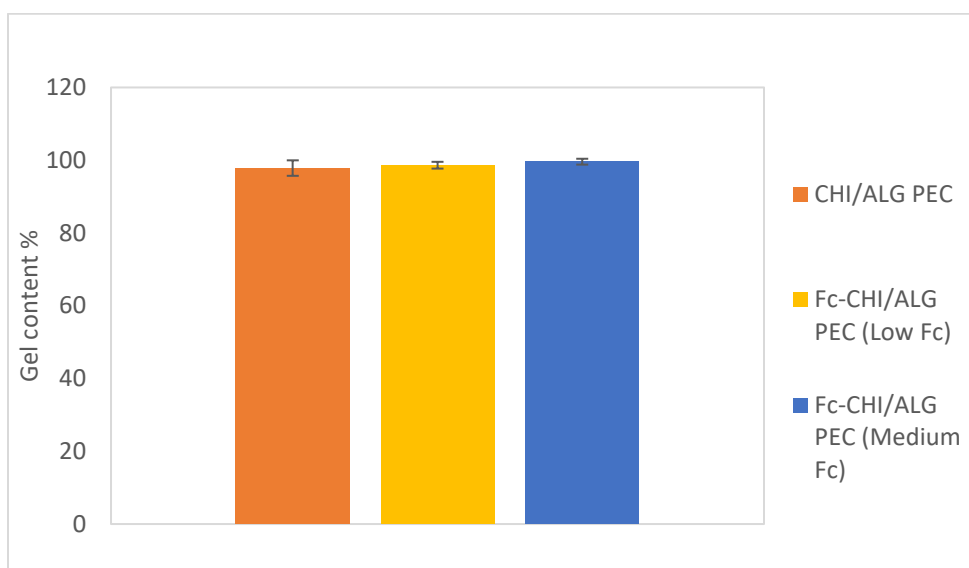
Figure 4.10. Gel content percentage of CHI/ALG, Fc-CHI/ALG (low Fc), and Fc-CHI/ALG (medium Fc) PEC hydrogels. The gel content test was performed on 3 samples and the average of the results was found and plotted.

4.3. Drug release studies

4.3.1. Drug release in solution

The release of FITC and FITC-D from CHI/ALG and Fc-CHI/ALG PEC hydrogels was investigated to evaluate their drug release behavior. Figure 4.11 shows the drug release behaviors of the PEC hydrogels loaded with FITC which has a relatively low molecular weight (332.3 g/mol). In 3 days, about 70% and 83% of the FITC were released, respectively, from CHI/ALG and Fc-CHI/ALG PEC hydrogels. The release rate

of FITC from CHI/ALG PEC hydrogel was lower due to the lesser amount of FITC molecules that were encapsulated into the CHI/ALG PEC hydrogel. This result may be explained by the swelling behavior that showed a lower swelling ratio for CHI/ALG PEC hydrogel among other PEC hydrogels. The drug release behavior can be also attributed to the strength of the ionic bond between the polyelectrolytes [64]. The ATR-FTIR shows that the ionic bond was stronger in CHI/ALG PEC, therefore the entrapped FITC may be released at a slower rate. It is likely that the electrostatic interaction between Fc-CHI and ALG in Fc-CHI/ALG PEC is lower due to the possible interaction of some of the amine groups on CHI with Fc, resulting in a faster release rate of the loaded FITC molecules.
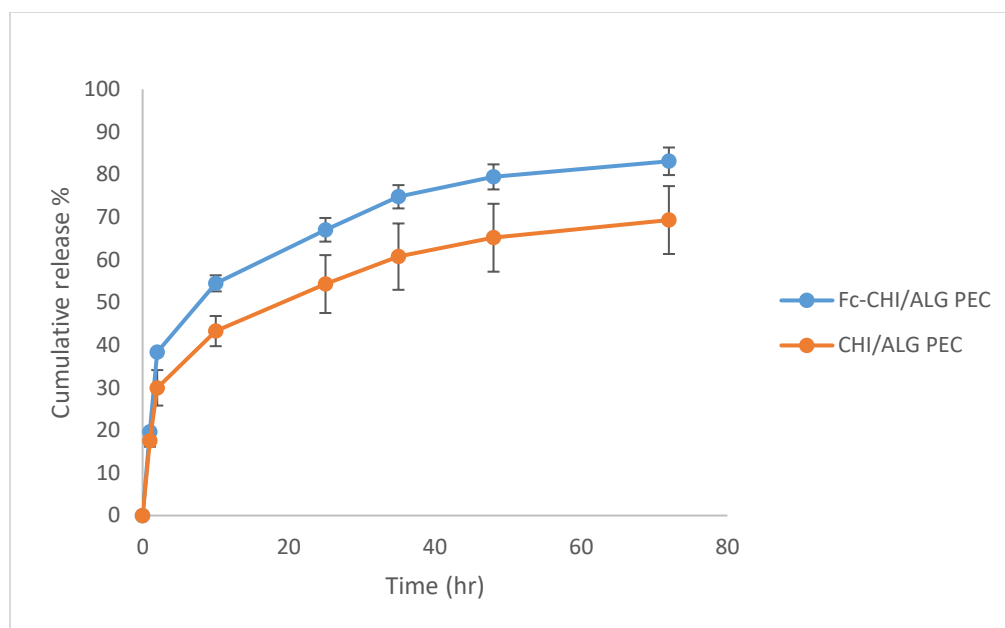
Figure 4.11. The cumulative release of FITC from CHI/ALG and Fc-CHI/ALG PEC hydrogels.

The release of FITC-D (a model drug with a large molecular weight of 2000-3000 Da) from the PEC hydrogels was also investigated in order to test the drug release behavior of the PEC hydrogels with two different model drugs with different molecular weights. As shown in Figure 4.12 about 38% and 61% of the FITC-D were released, respectively, from CHI/ALG and Fc-CHI/ALG PEC hydrogels over a period of 3 days. The results showed a similar trend as the FITC release in Figure 4.11. However, a slower

drug release rate from both PEC hydrogels was observed due to the larger molecular weight of the model drug, compared to FITC. Therefore, a smaller amount of the model drug was encapsulated into the PEC hydrogels and a slower release rate was observed.
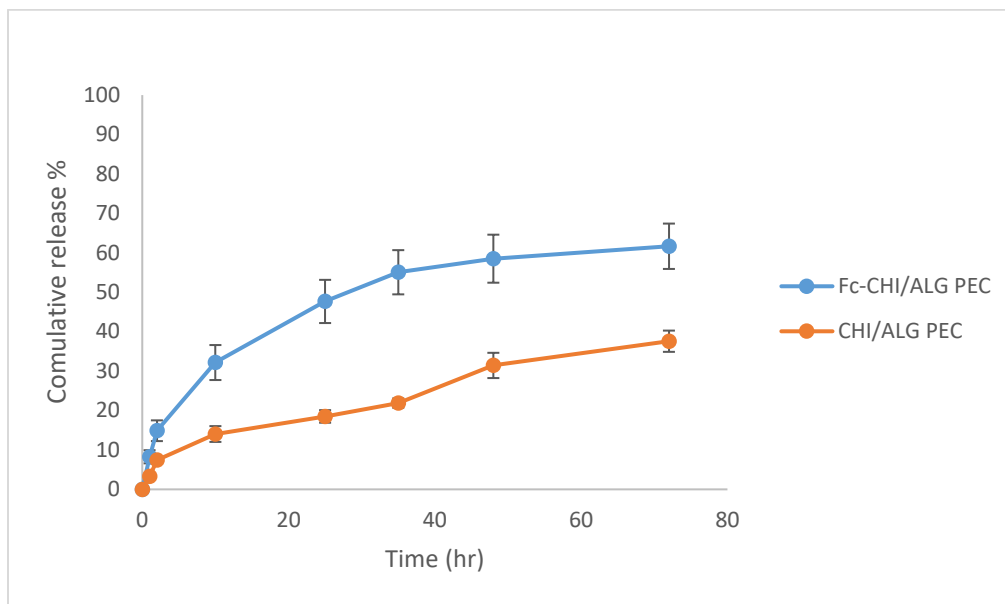
Figure 4.12. The cumulative release of FITC-D from CHI/ALG and Fc-CHI/ALG PEC hydrogels.

4.3.2. Drug release on the surface

The drug release kinetics of the PEC hydrogels were investigated on the surface of agarose gel to represent a similar condition to the wound site. The time-lapse images of the movement of the model drugs through agarose gel were collected (at the interface between the PEC hydrogels and agarose gel) for testing CHI/ALG and Fc-CHI/ALG PEC hydrogels in passive (no electrical stimulus) and active (with electrical stimulus) manners. To provide a sample of the images, the time-lapse images of the movement of FITC through agarose gel from Fc-CHI/ALG PEC in passive and active manners are shown in Figure 4.13. The figure clearly shows the enhanced release of the model drug with electrical stimulus, represented by the significant increase of the intensity of FITC that diffuses through the agarose gel with time. Also, these images were analyzed to find the change in the intensity profiles of the model drugs with time. The charts in Figures 4.13 and 4.14 show the spatiotemporal changes in the fluorescence intensity of FITC and FITC-

D, respectively, within the bulk agarose gel (phantom skin). Large deviations were observed in the collected data due to variations in the samples of the PEC hydrogels from batch to batch.
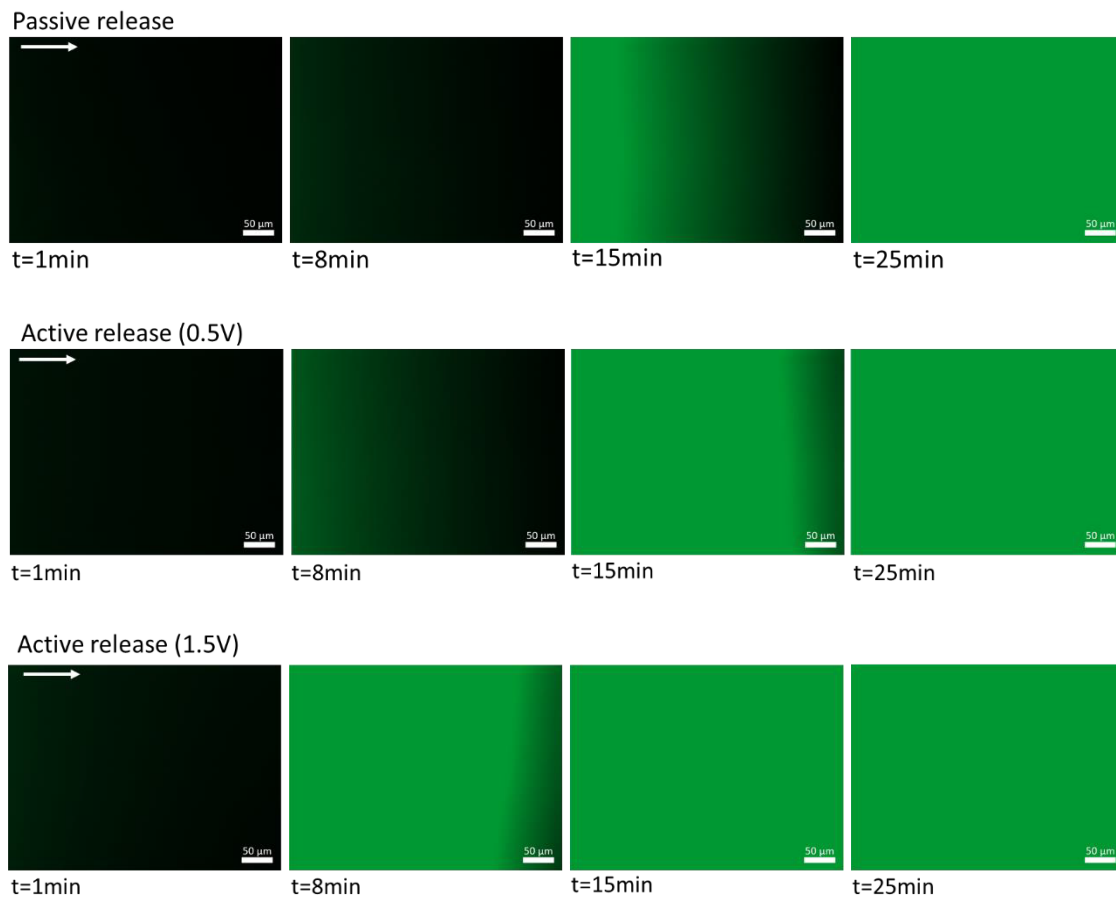
Figure 4.13. Images of the movement of FITC (released from Fc-CHI/ALG PEC) through agarose gel with no electrical stimulus and with an electrical stimulus (0.5V and 1.5V). (Scale bar 50µm)
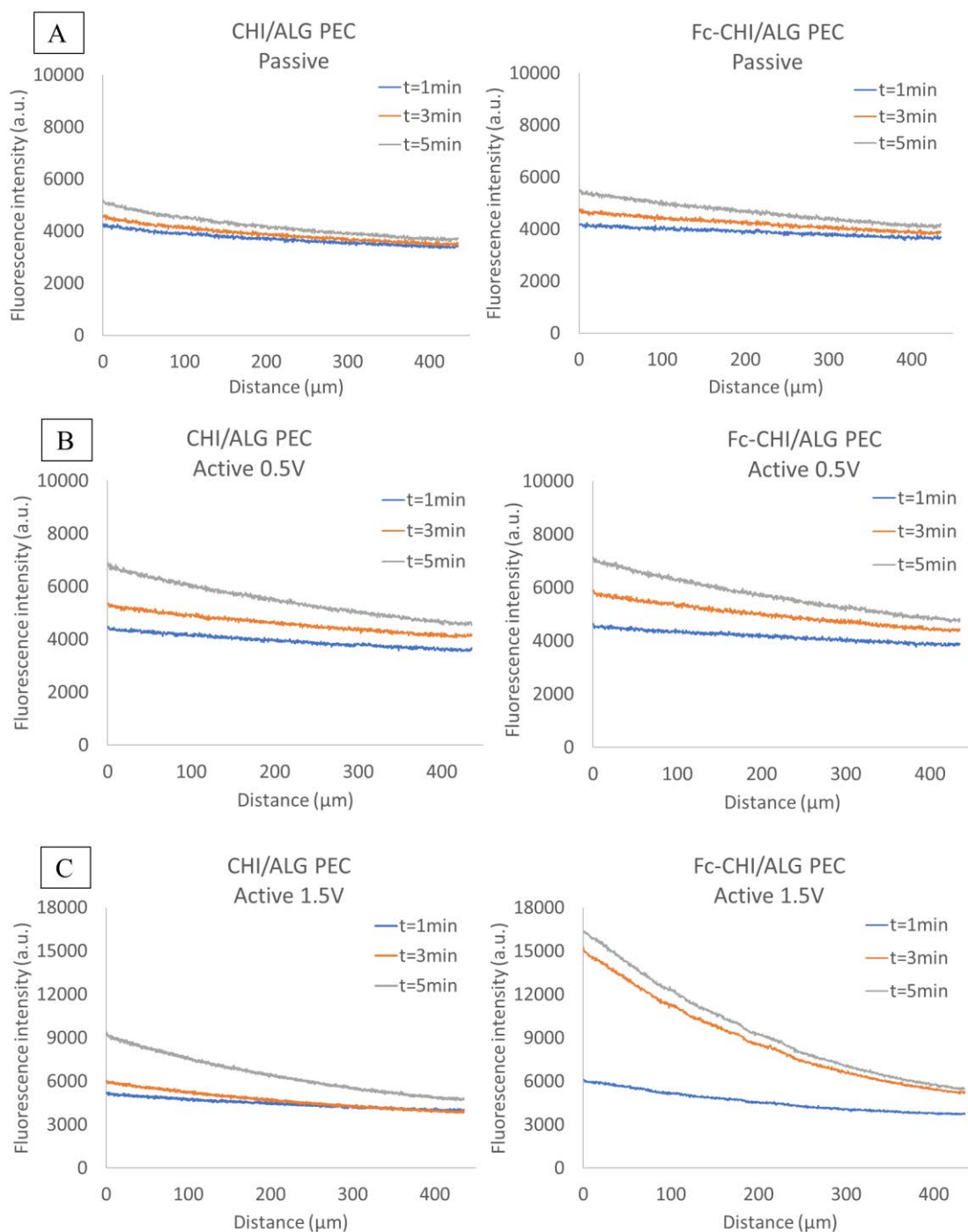
Figure 4.14. The change in the intensity profiles of FITC with time in passive release (A), active release 0.5V (B), and active release 1.5V (C) for CHI/ALG and Fc-CHI/ALG PEC hydrogels. (The plotted data is the average of 3 trials)
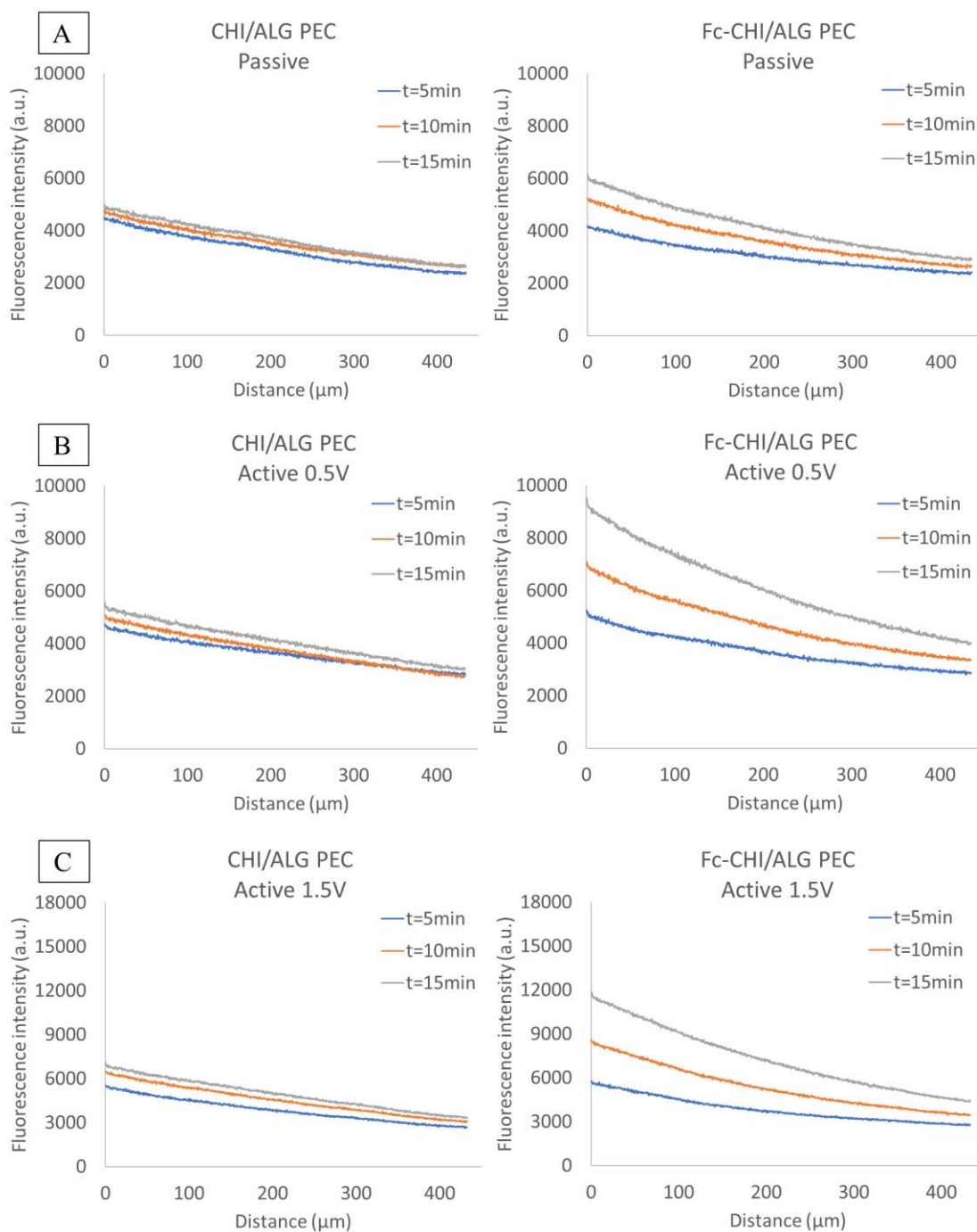
Figure 4.15. The change in the intensity profiles of FITC-D with time in passive release (A), active release 0.5V (B), and active release 1.5V (C) for CHI/ALG and Fc-CHI/ALG PEC hydrogels. (The plotted data is the average of 3 trials)

With no electrical stimulus, the passive release of FITC-D through agarose gel was slower compared to FITC release, which can be seen in Figures 4.14 and 4.15 (A). By comparing the intensity values at the interface to be 5500 a.u. for FITC and 4200 a.u. for FITC-D at the same time (5min), the lower intensity proves the slower release of FITC-D, which refers to the larger molecular weight. Therefore, a slower release rate from the PEC hydrogels is expected with the FITC-D.

Upon the electrical stimulus, both PEC hydrogels (CHI/ALG and Fc-CHI/ALG) were shown to be electrically responsive. The changes in the fluorescence intensity at the interface under the electrical stimulus were found to be larger than those in no electrical stimulus (see Figures 4.14 and 4.15). Also, it was found that the degree of the electrical potential (0.5 or 1.5 V) directly affects the release kinetics, resulting in changes in the fluorescence intensity. As shown in Figures 4.14 and 4.15 (B) and (C), a significant increase in the intensity values (16000 a.u. at t=5min) for the active release,1.5V compared to the intensity values (7000 a.u. at t=5min) for the active release,0.5 V. This result can be explained by the enhanced electro-osmosis that resulted from the higher electrical stimulus, therefore a faster drug release occurred (presented as higher intensity values).

To compare the electro-responsivity between the PEC hydrogels (CHI/ALG and Fc-CHI/ALG), Figure 4.16 shows the differences in the intensity profiles between both hydrogels at a specific time, for passive and active releases. The intensity values were found to be higher with the Fc-CHI/ALG PEC hydrogel with the electrical stimulus, indicating that it is more responsive to the electric field. This result may be attributed to the redox mediator of ferrocene that increases the electro-osmosis and the development of a stress gradient in the PEC hydrogel, therefore enhancing the release rate.
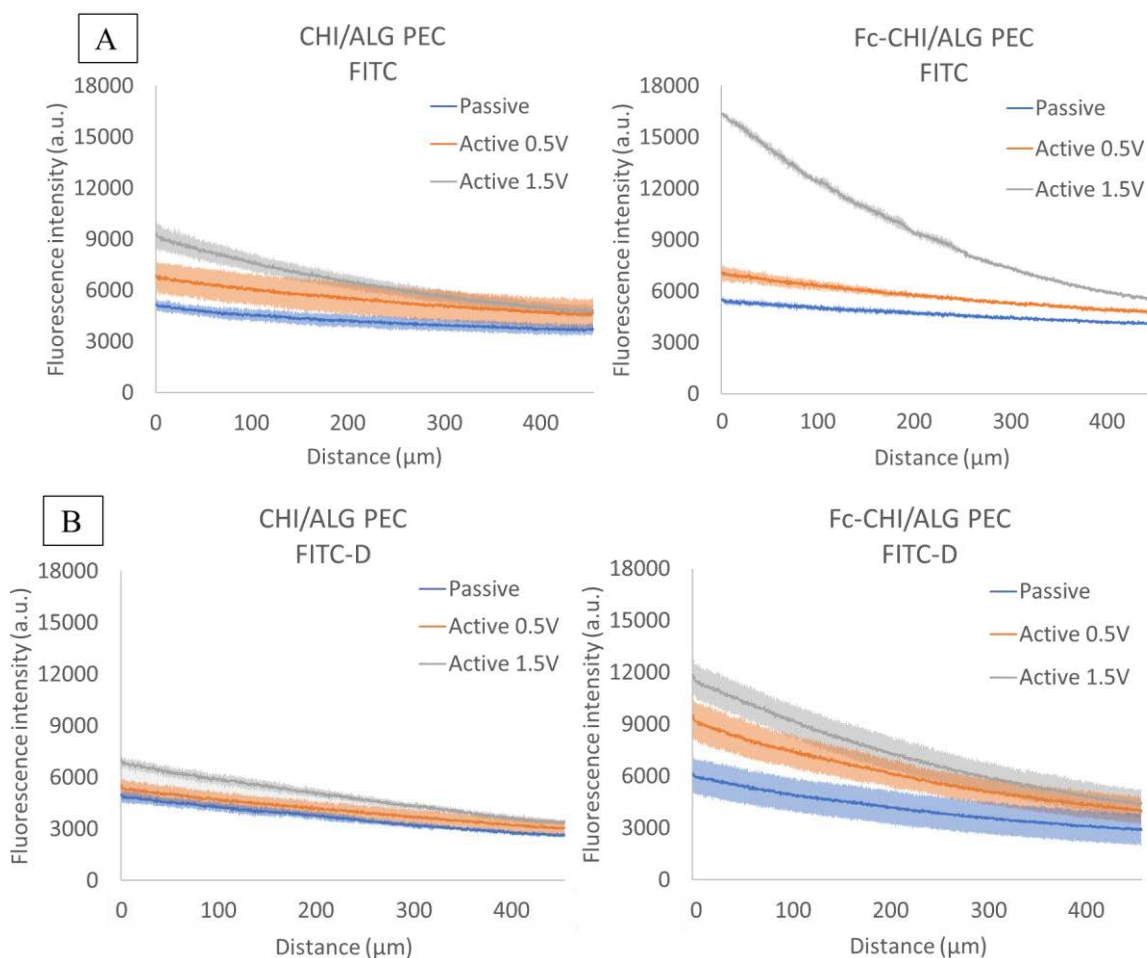
Figure 4.16. The intensity profiles for passive release and active releases under two different values of voltage (0.5V and 1.5V) for CHI/ALG and Fc-CHI/ALG PEC. (A) for FITC at t=5min. (B) for FITC-D at t=15min.

As mentioned in section 2.3.3.2, the condition of the functional groups of the polyelectrolytes plays a major role in the electro-responsivity of PEC hydrogels. The proposed mechanism of the electro-responsivity of the PEC hydrogels in this work is explained as follows: When the voltage is applied, a local decrease of the pH occurs around the anode and a neutral pH around the cathode [94]. The free amine groups available in the CHI/ALG PEC hydrogel are protonated, and the carboxyl groups available in the PEC hydrogel are neutralized on the anode side that is due to the low pH. On the cathode side, however, the carboxyl groups are deprotonated, and the amine groups are neutralized. Thus, the protonated amine groups would be attracted to the

cathode side, whereas the negatively charged carboxyl groups are attracted to the anode side. The result is that the   model drug is pushed out and an active release occurs.

With the Fc-CHI/ALG PEC hydrogel, the enhanced electro-responsivity compared to the CHI/ALG PEC hydrogel can be explained as shown in the schematic diagram in Figure 4.17. Ferrocene is a well-known organometallic redox couple (ferrocenium/ferrocene, Fc+/Fc) mediator that undergoes one-electron oxidation at a certain potential. Upon the electrical stimulus, the oxidized ferrocene (ferrocenium) together with the protonated amine groups of CHI would have a higher density of the protonated functional groups in the PEC hydrogel compared to the deprotonated carboxyl groups. The relatively larger amount of the positively charged functional groups on the cathode side may provide a higher electro-osmosis followed by a higher-pressure gradient in the PEC hydrogel. The enhanced driving force may induce the model drug molecules released more at the cathode side, compared to the case of the CHI/ALG PEC hydrogel with no ferrocene.
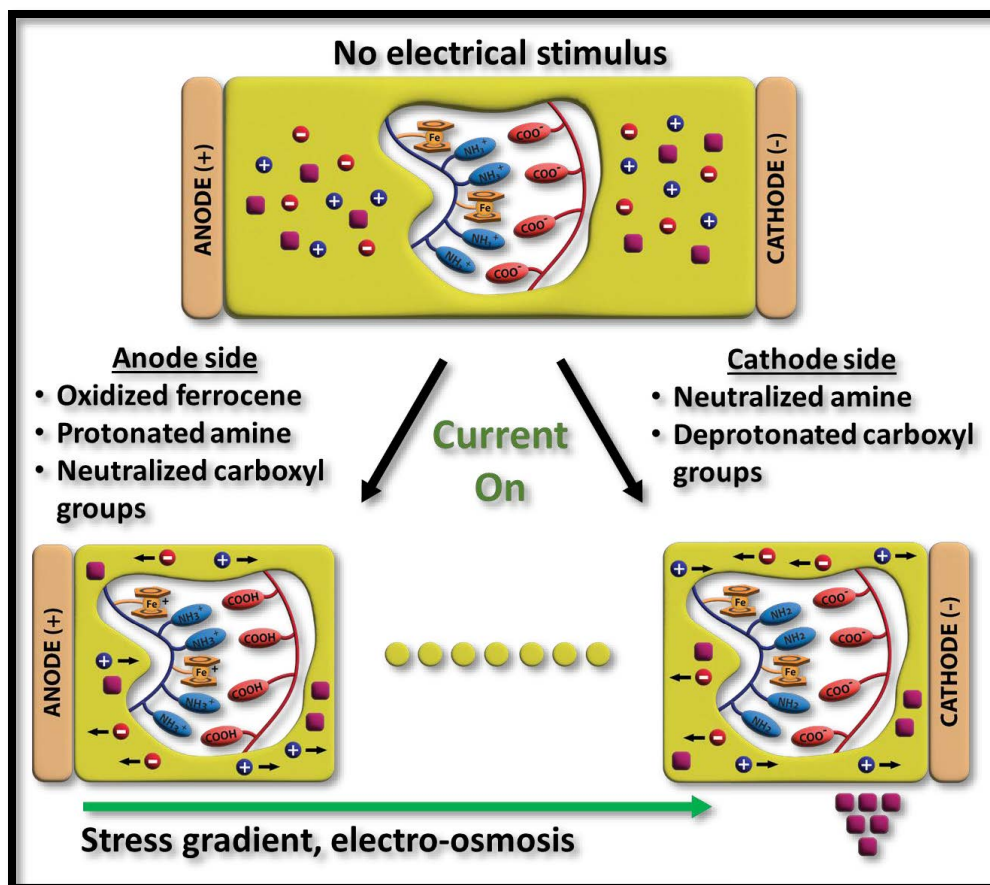
Figure 4.17. Schematic diagram of the mechanism of Fc-CHI/ALG PEC hydrogel electro-responsivity.

4.4. Diffusion coefficient calculations

The diffusion coefficients (D) of the passive and active releases were estimated by fitting the intensity profiles with an appropriate model based on the solution of Fick's second law (as mentioned in section 3.6). The D values obtained from different intensity profile curves at different times (for Fc-CHI/ALG PEC and FITC as a model drug) are summarized in Table 4.2. According to a previous study that applied the model to estimate D values [88], the D of the model drug should be constant at the different early times of diffusion. Moreover, another study demonstrated the estimation of D for various biomacromolecules diffused into a hydrogel-tissue matrix that has the same porosity. It was found that the apparent diffusion coefficients depend on the size of the biomacromolecules. The estimated D values should be similar and constant for one

specific molecular weight of the model drug (e.g., FITC or FITC-D in our study) [95]. However, despite maintaining a constant porosity of the diffusion media (a constant concentration of 2% w/v of agarose gel in our study), it's shown, in table 4.2, that the deviation of the estimated D values is large. The apparent diffusion coefficients were found to be 63.3, 14.3, and 5.7 m^2/s for passive release, 60.9, 12.2, and 4.2 m^2/s for active release (0.5V), and 15.8, 2.1, and 1.2 m^2/s for active release (1.5V) at the different incubation times of 1, 3, and 5 minutes, respectively. It is likely that the experimental setup for time-lapse imaging at a micro-scale may be challenging and provide a large deviation resulting from different imaging conditions and possible human error.

Figure 4.28 shows that the averaged D values for the different time points were found to be 27.7 ± 31.0, 25.7 ± 31.0, and 6.4 ± 8.0 m^2/s for passive, active 0.5V, and active 1.5V releases. The apparent D values with the large deviations indicate there is no statistically significant difference between the averaged D values. The number of experiments needs to increase so that the statistical analysis is carried out properly. Based on the results from the previous studies and our experimental result, it is confirmed that the estimated D values should be constant, regardless of the different amounts of the model drug released from the PEC hydrogels.

Table 4.2. Parameters P_1 and P_2 from Equation 3-7 and the estimated apparent diffusion coefficient values (D) for passive and active conditions at different times.

		Time (min)		
		1	**3**	**5**
Passive, 0V	P_1	4055 ± 50	4481 ± 137	5099 ± 223
	$P_2 \times 10^7$	6.8 ± 1.4	10 ± 1.6	15 ± 1.4
	$D \times 10^{10}\,(\mathrm{m^2/s})$	63.3	14.3	5.7
	$SD \times 10^{10}$	12.1	2.4	0.5
Active, 0.5V	P_1	4387 ± 253	4970 ± 277	6179 ± 298
	$P_2 \times 10^7$	8.5 ± 3.8	1.2 ± 4.2	20.4 ± 4.17
	$D \times 10^{10}\,(\mathrm{m^2/s})$	60.9	12.2	4.2
	$SD \times 10^{10}$	28.2	3.5	0.8
Active, 1.5V	P_1	5380 ± 133	12426 ± 678	13601 ± 300
	$P_2 \times 10^7$	26.5 ± 144	65.7 ± 1.7	68.8 ± 1.1
	$D \times 10^{10}\,(\mathrm{m^2/s})$	15.8	2.1	1.2
	$SD \times 10^{10}$	0.89	0.06	0.02
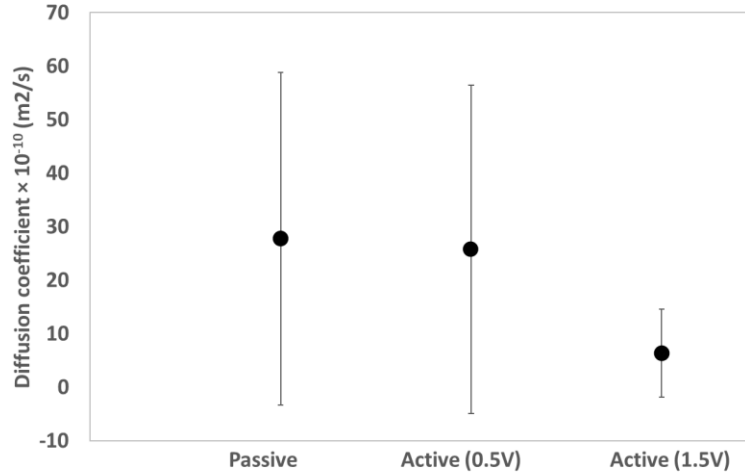
Figure 4.18. The apparent diffusion coefficient values.

5. Conclusions and recommendations

This work presented the importance of the PEC hydrogels as drug carriers for smart wound dressings. Natural and electro-responsive PEC hydrogel composed of Fc-CHI and ALG was obtained and characterized. The hydrogel showed promising results for smart wound dressing application. Conclusions of this thesis, as well as future research and improvements to this work, are presented below:

- The CHI/ALG PEC hydrogel (no ferrocene) was obtained and used as a control.

- According to the turbidity test the optimum ratio of the polyelectrolytes was (20% CHI,80% ALG) and (25% CHI,75% ALG) for CHI/ALG and Fc-CHI/ALG PEC hydrogels, respectively.

- The turbidity increased up to polycation/polyanion (CHI/ALG) ratios close to the theoretical neutralization point of the polyelectrolytes, and decreased after this ratio was exceeded. The peak shift in the turbidity chart was attributed to the less amount of amine groups of CHI as the amount of Fc conjugated into the CHI increased. A larger amount of Fc-CHI (polycation) was needed in order to neutralize the ALG (polyanionic) charge.

- The stronger ionic interaction was observed with the CHI/ALG PEC than the Fc-CHI/ALG PEC, which was proved by the ATR-FTIR analysis.

- The EDS analysis confirmed the synthesis of Fc-CHI was successful, which was proved by the peak representing iron (Fe) sandwiched between two cyclopentadienyl rings in staggered conformation of ferrocene.

- The CHI/ALG PEC swelling percentage was found to be 3480%, while the swelling percentage of Fc-CHI/ALG PEC reached 4471%, which proves more preferable swelling behavior.

- The PEC hydrogel showed good stability, which was supported by the result that the hydrogel has almost 100% gel content.

- When it comes to the drug release kinetics in solution, after 3 days of incubation, about 70% of the incubated FITC was released from CHI/ALG PEC, while 83% was released from Fc-CHI/ALG PEC. Similarly, in the same period of time, 38% of the

incubated FITC-D was released from CHI/ALG PEC and 61% from Fc-CHI/ALG PEC.

- The Fc-CHI/ALG PEC hydrogel showed more electro-responsivity than the CHI/ALG PEC hydrogel. The Fc-CHI/ALG PEC hydrogel showed enhanced electro-responsivity; a faster release of the model drugs was observed upon the electrical stimulus.

- The time-lapse images showing the diffusion of the model drug at the interface between the agarose gel and the PEC hydrogels proved the electro-responsivity of the PEC hydrogels by showing a significant increase in the model drug intensity with time, upon the electrical stimulus. A drug release under a voltage of 1.5V was faster than that of 0.5V.

- The experimental deviations were observed in the drug release kinetic study on the surface, which might be due to the changes in the PEC hydrogel samples from batch to batch. A homogenizer needs to be used to overcome this condition.

- The estimated diffusion coefficients were calculated to be 27.7 ± 31.0, 25.7 ± 31.0, and 6.4 ± 8.0 m^2/s for passive, active 0.5V, and active 1.5V releases, respectively, the apparent D values with the large deviations, indicating there is no statistically significant difference between the averaged D values. The number of the experiment al trials needs to be increased so that the statistical analysis is carried out properly. Based on the results from the previous studies and our experimental result, it is confirmed that the estimated D values should be constant, regardless of the different amounts of the model drug released from the PEC hydrogels.

- The controlled release of the model drugs under the electrical stimulus may provide more efficient therapy by reducing side effects and enhancing patient compliance.

- For future work, an *in vitro* test of the developed electrically-responsive PEC hydrogel is required to estimate an antibacterial releasing of the PEC hydrogel.

References

1. Jiang, H., et al., *A pH-regulated drug delivery dermal patch for targeting infected regions in chronic wounds.* Lab on a Chip, 2019. **19**(13): p. 2265-2274.
2. Dhivya, S., V.V. Padma, and E. Santhini, *Wound dressings–a review.* BioMedicine, 2015. **5**(4): p. 1-5.
3. Ovington, L.G., *Advances in wound dressings.* Clinics in dermatology, 2007. **25**(1): p. 33-38.
4. Farahani, M. and A. Shafiee, *Wound healing: From passive to smart dressings.* Advanced Healthcare Materials, 2021. **10**(16): p. 2100477.
5. Catanzano, O., F. Quaglia, and J.S. Boateng, *Wound dressings as growth factor delivery platforms for chronic wound healing.* Expert Opinion on Drug Delivery, 2021: p. 1-23.
6. Dong, R. and B. Guo, *Smart wound dressings for wound healing.* Nano Today, 2021. **41**: p. 101290.
7. Bagherifard, S., et al., *Dermal patch with integrated flexible heater for on demand drug delivery.* Advanced healthcare materials, 2016. **5**(1): p. 175-184.
8. Liu, L., et al., *A pH-Indicating colorimetric tough hydrogel patch towards applications in a substrate for smart wound dressings.* Polymers, 2017. **9**(11): p. 558.
9. Ajovalasit, A., et al., *Development and characterization of xyloglucan-poly (vinyl alcohol) hydrogel membrane for Wireless Smart wound dressings.* European Polymer Journal, 2018. **106**: p. 214-222.
10. Rezaei, N., et al., *Antimicrobial peptides-loaded smart chitosan hydrogel: Release behavior and antibacterial potential against antibiotic resistant clinical isolates.* International Journal of Biological Macromolecules, 2020. **164**: p. 855-862.
11. Hoare, T.R. and D.S. Kohane, *Hydrogels in drug delivery: Progress and challenges.* Polymer, 2008. **49**(8): p. 1993-2007.
12. Bahram, M., N. Mohseni, and M. Moghtader, *An introduction to hydrogels and some recent applications*, in *Emerging concepts in analysis and applications of hydrogels*. 2016, IntechOpen.
13. Peppas, N.A. and A.S. Hoffman, *Hydrogels*, in *Biomaterials science*. 2020, Elsevier. p. 153-166.
14. Pogodina, N.V. and N.V. Tsvetkov, *Structure and dynamics of the polyelectrolyte complex formation.* Macromolecules, 1997. **30**(17): p. 4897-4904.
15. Kwon, I.C., Y.H. Bae, and S.W. Kim, *Heparin release from polymer complex.* Journal of controlled release, 1994. **30**(2): p. 155-159.
16. Yoshizawa, T., et al., *pH-and temperature-sensitive release behaviors from polyelectrolyte complex films composed of chitosan and PAOMA copolymer.* European journal of pharmaceutics and biopharmaceutics, 2005. **59**(2): p. 307-313.
17. Hu, X., et al., *Triggered release of encapsulated cargo from photoresponsive polyelectrolyte nanocomplexes.* ACS applied materials & interfaces, 2016. **8**(36): p. 23517-23522.

18. Chu, C.-H., T. Sakiyama, and T. Yano, *pH-sensitive swelling of a polyelectrolyte complex gel prepared from xanthan and chitosan.* Bioscience, biotechnology, and biochemistry, 1995. **59**(4): p. 717-719.

19. Kim, S.J., et al., *Electrical/pH-sensitive swelling behavior of polyelectrolyte hydrogels prepared with hyaluronic acid–poly (vinyl alcohol) interpenetrating polymer networks.* Reactive and Functional Polymers, 2003. **55**(3): p. 291-298.

20. Islam, S., M. Bhuiyan, and M. Islam, *Chitin and chitosan: structure, properties and applications in biomedical engineering.* Journal of Polymers and the Environment, 2017. **25**(3): p. 854-866.

21. Kas, H.S., *Chitosan: properties, preparations and application to microparticulate systems.* Journal of microencapsulation, 1997. **14**(6): p. 689-711.

22. Yang, J.-S., Y.-J. Xie, and W. He, *Research progress on chemical modification of alginate: A review.* Carbohydrate polymers, 2011. **84**(1): p. 33-39.

23. Lee, K.Y. and D.J. Mooney, *Alginate: properties and biomedical applications.* Progress in polymer science, 2012. **37**(1): p. 106-126.

24. Gierszewska, M., J. Ostrowska-Czubenko, and E. Chrzanowska, *pH-responsive chitosan/alginate polyelectrolyte complex membranes reinforced by tripolyphosphate.* European Polymer Journal, 2018. **101**: p. 282-290.

25. Qiu, J.-D., et al., *A label-free amperometric immunosensor based on biocompatible conductive redox chitosan-ferrocene/gold nanoparticles matrix.* Biosensors and Bioelectronics, 2009. **25**(4): p. 852-857.

26. Yılmaz, Ö., et al., *Chitosan–ferrocene film as a platform for flow injection analysis applications of glucose oxidase and Gluconobacter oxydans biosensors.* Colloids and Surfaces B: Biointerfaces, 2012. **100**: p. 62-68.

27. Schultz, G.S., et al., *Wound bed preparation: a systematic approach to wound management.* Wound repair and regeneration, 2003. **11**: p. S1-S28.

28. Rezvani Ghomi, E., et al., *Wound dressings: Current advances and future directions.* Journal of Applied Polymer Science, 2019. **136**(27): p. 47738.

29. Saco, M., et al., *Comparing the efficacies of alginate, foam, hydrocolloid, hydrofiber, and hydrogel dressings in the management of diabetic foot ulcers and venous leg ulcers: a systematic review and meta-analysis examining how to dress for success.* Dermatology online journal, 2016. **22**(8).

30. Wathoni, N., et al., *Physically crosslinked-sacran hydrogel films for wound dressing application.* International journal of biological macromolecules, 2016. **89**: p. 465-470.

31. Tsao, C.T., et al., *Evaluation of chitosan/γ-poly (glutamic acid) polyelectrolyte complex for wound dressing materials.* Carbohydrate polymers, 2011. **84**(2): p. 812-819.

32. Balakrishnan, B., et al., *Evaluation of an in situ forming hydrogel wound dressing based on oxidized alginate and gelatin.* Biomaterials, 2005. **26**(32): p. 6335-6342.

33. Jantrawut, P., et al., *Fabrication and characterization of low methoxyl pectin/gelatin/carboxymethyl cellulose absorbent hydrogel film for wound dressing applications.* Materials, 2019. **12**(10): p. 1628.

34. Ehterami, A., et al., *A promising wound dressing based on alginate hydrogels containing vitamin D3 cross-linked by calcium carbonate/d-glucono-δ-lactone.* Biomedical Engineering Letters, 2020. **10**(2): p. 309.

35. Salehi, M., et al., *Accelerating healing of excisional wound with alginate hydrogel containing naringenin in rat model.* Drug Delivery and Translational Research, 2021. **11**(1): p. 142-153.

36. Ahmed, A.S., et al., *PVA-PEG physically cross-linked hydrogel film as a wound dressing: experimental design and optimization.* Pharmaceutical development and technology, 2018. **23**(8): p. 751-760.

37. Rezvanian, M., et al., *Optimization, characterization, and in vitro assessment of alginate-pectin ionic cross-linked hydrogel film for wound dressing applications.* International journal of biological macromolecules, 2017. **97**: p. 131-140.

38. Haidari, H., et al., *pH-Responsive "Smart" Hydrogel for Controlled Delivery of Silver Nanoparticles to Infected Wounds.* Antibiotics, 2021. **10**(1): p. 49.

39. Pang, Q., et al., *Smart flexible electronics-integrated wound dressing for real-time monitoring and on-demand treatment of infected wounds.* Advanced Science, 2020. **7**(6): p. 1902673.

40. Kuo, S.-H., et al., *Role of pH value in clinically relevant diagnosis.* Diagnostics, 2020. **10**(2): p. 107.

41. Richbourg, N.R. and N.A. Peppas, *The swollen polymer network hypothesis: Quantitative models of hydrogel swelling, stiffness, and solute transport.* Progress in Polymer Science, 2020. **105**: p. 101243.

42. Colombo, P., *Swelling-controlled release in hydrogel matrices for oral route.* Advanced Drug Delivery Reviews, 1993. **11**(1-2): p. 37-57.

43. Fumio, U., et al., *Swelling and mechanical properties of poly (vinyl alcohol) hydrogels.* International journal of pharmaceutics, 1990. **58**(2): p. 135-142.

44. Briones, A.V. and T. Sato, *Encapsulation of glucose oxidase (GOD) in polyelectrolyte complexes of chitosan–carrageenan.* Reactive and Functional Polymers, 2010. **70**(1): p. 19-27.

45. Gunatillake, P.A., R. Adhikari, and N. Gadegaard, *Biodegradable synthetic polymers for tissue engineering.* Eur Cell Mater, 2003. **5**(1): p. 1-16.

46. García-Astrain, C., et al., *Biocompatible hydrogel nanocomposite with covalently embedded silver nanoparticles.* Biomacromolecules, 2015. **16**(4): p. 1301-1310.

47. Taghipour, Y.D., et al., *The application of hydrogels based on natural polymers for tissue engineering.* Current medicinal chemistry, 2020. **27**(16): p. 2658-2680.

48. Stanton, M., J. Samitier, and S. Sanchez, *Bioprinting of 3D hydrogels.* Lab on a Chip, 2015. **15**(15): p. 3111-3115.

49. Hao, Y., et al., *Bio-multifunctional alginate/chitosan/fucoidan sponges with enhanced angiogenesis and hair follicle regeneration for promoting full-thickness wound healing.* Materials & Design, 2020. **193**: p. 108863.

50. Zhang, Y.S. and A. Khademhosseini, *Advances in engineering hydrogels.* Science, 2017. **356**(6337): p. eaaf3627.

51. Lee, C.-T., P.-H. Kung, and Y.-D. Lee, *Preparation of poly (vinyl alcohol)-chondroitin sulfate hydrogel as matrices in tissue engineering.* Carbohydrate Polymers, 2005. **61**(3): p. 348-354.

52. Ma, C., et al., *Mammalian and fish gelatin methacryloyl–alginate interpenetrating polymer network hydrogels for tissue engineering.* ACS omega, 2021. **6**(27): p. 17433-17441.

53. Sosnik, A. and M.V. Sefton, *Semi-synthetic collagen/poloxamine matrices for tissue engineering.* Biomaterials, 2005. **26**(35): p. 7425-7435.

54. Du, J., et al., *Novel pH-sensitive polyelectrolyte carboxymethyl Konjac glucomannan-chitosan beads as drug carriers.* Reactive and Functional Polymers, 2006. **66**(10): p. 1055-1061.

55. Hamman, J.H., *Chitosan based polyelectrolyte complexes as potential carrier materials in drug delivery systems.* Marine drugs, 2010. **8**(4): p. 1305-1322.

56. Zhu, T., et al., *Metallo-polyelectrolytes as a class of ionic macromolecules for functional materials.* Nature communications, 2018. **9**(1): p. 1-15.

57. Berger, J., et al., *Structure and interactions in covalently and ionically crosslinked chitosan hydrogels for biomedical applications.* European journal of pharmaceutics and biopharmaceutics, 2004. **57**(1): p. 19-34.

58. Feng, X., R. Pelton, and M. Leduc, *Mechanical properties of polyelectrolyte complex films based on polyvinylamine and carboxymethyl cellulose.* Industrial & engineering chemistry research, 2006. **45**(20): p. 6665-6671.

59. Park, J.W., K.H. Park, and S. Seo, *Natural polyelectrolyte complex-based pH-dependent delivery carriers using alginate and chitosan.* Journal of Applied Polymer Science, 2019. **136**(43): p. 48143.

60. Kulig, D., et al., *Study on alginate–chitosan complex formed with different polymers ratio.* Polymers, 2016. **8**(5): p. 167.

61. Sæther, H.V., et al., *Polyelectrolyte complex formation using alginate and chitosan.* Carbohydrate Polymers, 2008. **74**(4): p. 813-821.

62. Ankerfors, C., et al., *Using jet mixing to prepare polyelectrolyte complexes: Complex properties and their interaction with silicon oxide surfaces.* Journal of colloid and interface science, 2010. **351**(1): p. 88-95.

63. Il'Ina, A. and V. Varlamov, *Chitosan-based polyelectrolyte complexes: a review.* Applied Biochemistry and Microbiology, 2005. **41**(1): p. 5-11.

64. Dai, M., et al., *Chitosan-alginate sponge: preparation and application in curcumin delivery for dermal wound healing in rat.* Journal of Biomedicine and Biotechnology, 2009. **2009**.

65. Kulkarni, A.D., et al., *Polyelectrolyte complexes: mechanisms, critical experimental aspects, and applications.* Artificial cells, nanomedicine, and biotechnology, 2016. **44**(7): p. 1615-1625.

66. Strand, A., et al., *In-situ analysis of polyelectrolyte complexes by flow cytometry.* Cellulose, 2018. **25**(7): p. 3781-3795.

67. Meka, V.S., et al., *A comprehensive review on polyelectrolyte complexes.* Drug discovery today, 2017. **22**(11): p. 1697-1706.

68. Potaś, J., et al., *Tragacanth Gum/Chitosan Polyelectrolyte Complexes-Based Hydrogels Enriched with Xanthan Gum as Promising Materials for Buccal Application.* Materials, 2021. **14**(1): p. 86.

69. Kulkarni Vishakha, S., D. Butte Kishor, and S. Rathod Sudha, *Natural polymers– A comprehensive review.* International journal of research in pharmaceutical and biomedical sciences, 2012. **3**(4): p. 1597-1613.

70. Dautzenberg, H., et al., *Development of cellulose sulfate-based polyelectrolyte complex microcapsules for medical applications.* Annals of the New York Academy of Sciences, 1999. **875**(1): p. 46-63.

71. Kilicarslan, M., et al., *Preparation and evaluation of clindamycin phosphate loaded chitosan/alginate polyelectrolyte complex film as mucoadhesive drug delivery system for periodontal therapy.* European Journal of Pharmaceutical Sciences, 2018. **123**: p. 441-451.

72. Arora, S., et al., *Amoxicillin loaded chitosan–alginate polyelectrolyte complex nanoparticles as mucopenetrating delivery system for H. pylori.* Scientia pharmaceutica, 2011. **79**(3): p. 673-694.

73. Armenta-Rojas, E., et al., *Nystatin-loaded Polyelectrolyte Complex Films as a Mucoadhesive Drug Delivery System for Potential Buccal Application.* Biointerface Res. Appl. Chem, 2022. **12**: p. 4384-4398.

74. Chen, L., et al., *Novel hyaluronic acid coated hydrophobically modified chitosan polyelectrolyte complex for the delivery of doxorubicin.* International journal of biological macromolecules, 2019. **126**: p. 254-261.

75. Aswathy, S., U. Narendrakumar, and I. Manjubala, *Commercial hydrogels for biomedical applications.* Heliyon, 2020. **6**(4): p. e03719.

76. Maitz, M.F., *Applications of synthetic polymers in clinical medicine.* Biosurface and Biotribology, 2015. **1**(3): p. 161-176.

77. Liu, X., J.-P. Chapel, and C. Schatz, *Structure, thermodynamic and kinetic signatures of a synthetic polyelectrolyte coacervating system.* Advances in colloid and interface science, 2017. **239**: p. 178-186.

78. Yoon, D.M. and J.P. Fisher, *Natural and synthetic polymeric scaffolds*, in *Biomedical materials*. 2021, Springer. p. 257-283.

79. Shu, X. and K. Zhu, *A novel approach to prepare tripolyphosphate/chitosan complex beads for controlled release drug delivery.* International journal of pharmaceutics, 2000. **201**(1): p. 51-58.

80. Paloma, M., et al., *Release of amoxicillin from polyionic complexes of chitosan and poly (acrylic acid). Study of polymer/polymer and polymer/drug interactions within the network structure.* Biomaterials, 2003. **24**(8): p. 1499-1506.

81. Ahn, J.-S., et al., *Release of triamcinolone acetonide from mucoadhesive polymer composed of chitosan and poly (acrylic acid) in vitro.* Biomaterials, 2002. **23**(6): p. 1411-1416.

82. Gujarathi, N.A., B.R. Rane, and J.K. Patel, *pH sensitive polyelectrolyte complex of O-carboxymethyl chitosan and poly (acrylic acid) cross-linked with calcium for sustained delivery of acid susceptible drugs.* International journal of pharmaceutics, 2012. **436**(1-2): p. 418-425.

83. Nath, S.D., et al., *Chitosan–hyaluronic acid polyelectrolyte complex scaffold crosslinked with genipin for immobilization and controlled release of BMP-2.* Carbohydrate polymers, 2015. **115**: p. 160-169.

84. Li, G., et al., *Dually pH-responsive polyelectrolyte complex hydrogel composed of polyacrylic acid and poly (2-(dimthylamino) ethyl methacrylate).* Polymer, 2016. **107**: p. 332-340.

85. Malay, Ö., A. Batıgün, and O. Bayraktar, *pH-and electro-responsive characteristics of silk fibroin–hyaluronic acid polyelectrolyte complex membranes.* International journal of pharmaceutics, 2009. **380**(1-2): p. 120-126.

86. Shi, J., N.M. Alves, and J.F. Mano, *Chitosan coated alginate beads containing poly (N-isopropylacrylamide) for dual-stimuli-responsive drug release.* Journal of Biomedical Materials Research Part B: Applied Biomaterials: An Official Journal of The Society for Biomaterials, The Japanese Society for Biomaterials, and The Australian Society for Biomaterials and the Korean Society for Biomaterials, 2008. **84**(2): p. 595-603.

87. Recillas, M., et al., *Thermo-and pH-responsive polyelectrolyte complex membranes from chitosan-gN-isopropylacrylamide and pectin.* Carbohydrate polymers, 2011. **86**(3): p. 1336-1343.

88. Krupa, I., et al., *Glucose diffusivity and porosity in silica hydrogel based on organofunctional silanes.* European polymer journal, 2011. **47**(7): p. 1477-1484.

89. Floury, J., et al., *Diffusion of solutes inside bacterial colonies immobilized in model cheese depends on their physicochemical properties: a time-lapse microscopy study.* Frontiers in microbiology, 2015. **6**: p. 366.

90. Zhang, Y., et al., *The influence of ionic strength and mixing ratio on the colloidal stability of PDAC/PSS polyelectrolyte complexes.* Soft Matter, 2015. **11**(37): p. 7392-7401.

91. Yang, W., H. Zhou, and C. Sun, *Synthesis of ferrocene-branched chitosan derivatives: redox polysaccharides and their application to reagentless enzyme-based biosensors.* Macromolecular rapid communications, 2007. **28**(3): p. 265-270.

92. Chalitangkoon, J., M. Wongkittisin, and P. Monvisade, *Silver loaded hydroxyethylacryl chitosan/sodium alginate hydrogel films for controlled drug release wound dressings.* International Journal of Biological Macromolecules, 2020. **159**: p. 194-203.

93. Lin, K.-Y.A., J.-T. Lin, and H. Yang, *Ferrocene-modified chitosan as an efficient and green heterogeneous catalyst for sulfate-radical-based advanced oxidation process.* Carbohydrate polymers, 2017. **173**: p. 412-421.

94. Kulkarni, R. and S. Biswanath, *Electrically responsive smart hydrogels in drug delivery: a review.* Journal of applied biomaterials and biomechanics, 2007. **5**(3): p. 125-139.

95. Li, J., et al., *Fast immuno-labeling by electrophoretically driven infiltration for intact tissue imaging.* Scientific reports, 2015. **5**(1): p. 1-7.